3-22-2019

Two-On-One Pursuit with a Non-zero Capture Radius

Patrick J. Wasz

Two-On-One Pursuit with a Non-Zero Caputure Radius

THESIS

Patrick J. Wasz, Lt, USAF
AFIT/ENG/19M

DEPARTMENT OF THE AIR FORCE
AIR UNIVERSITY

AIR FORCE INSTITUTE OF TECHNOLOGY

Wright-Patterson Air Force Base, Ohio

AFIT/ENG/19M

TWO-ON-ONE PURSUIT WITH A NON-ZERO CAPUTURE RADIUS

THESIS

Presented to the Faculty

Department of Electrical and Computer Engineering

Graduate School of Engineering and Management

Air Force Institute of Technology

Air University

Air Education and Training Command

in Partial Fulfillment of the Requirements for the

Degree of Master of Science in Electrical Engineering

Patrick J. Wasz, BS

Lt, USAF

March 2019

AFIT/ENG/19M

TWO-ON-ONE PURSUIT WITH A NON-ZERO CAPUTURE RADIUS

THESIS

Patrick J. Wasz, BS
Lt, USAF

Committee Membership:

Meir Pacther, Ph.D
Chair

Robert C. Leishmann, Ph.D
Member

Capt. Joshuah A. Hess, Ph.D
Member

AFIT/ENG/19M

Abstract

In this paper, we revisit the "Two Cutters and Fugitive Ship" differential game that was addressed by Isaacs, but move away from point capture. We consider a two-on-one pursuit-evasion differential game with simple motion and pursuers endowed with circular capture sets of radius $l > 0$. The regions in the state space where only one pursuer effects the capture and the region in the state space where both pursuers cooperatively and isochronously capture the evader are characterized, thus solving the Game of Kind. Concerning the Game of Degree, the algorithm for the synthesis of the optimal state feedback strategies of the cooperating pursuers and of the evader is presented.

Acknowledgements

Anything begun in vanity ends in humility.

I'd like to thank my family, friends, and all of the great people that I've had the pleasure of working with over the past year. I've learned a great deal both in my studies and in life in general from all of you.

Patrick J. Wasz

Table of Contents

List of Figures

TWO-ON-ONE PURSUIT WITH

A NON-ZERO CAPUTURE RADIUS

I. Introduction

In this paper we consider a two-on-one pursuit-evasion differential game with simple motion and pursuers endowed with circular capture sets. We revisit the "Two Cutters and Fugitive Ship" differential game that was addressed by Isaacs [1], [2], but move away from point capture. The pursuers are now endowed with a radius of capture $l > 0$. The regions in the state space where only one pursuer effects the capture and the region in the state space where both pursuers cooperatively capture the evader are delineated and the algorithm for the synthesis of the optimal state feedback strategies of the cooperating pursuers and of the evader is presented. In this game, all players have simple motion and the evader/pursuer's speed ratio is $\mu \triangleq \frac{v_E}{v_P} < 1$. Thus, the problem parameters are μ and l. Because the pursuers are faster, the evader cannot escape if the pursuers play optimally.

We start by constructing the Safe Region (SR) and Boundary of the Safe Region (BSR) of the evader. This elemental BSR is the locus of points that the Evader (E) and a Pursuer (P) will reach at the same time along straight line trajectories. The construction of the elemental BSR in the case of point capture when $l = 0$ is based on the concept of the Apollonius circle. When the capture radius of the Pursuer $l > 0$, the BSR of E will be a Cartesian oval — we shall refer to these as "Apollonius ovals". This forms the basis for constructing the composite SR and BSR of E when two pursuers are at work. The introduction of a non-zero radius of capture affects the geometry of the surface in the state space which separates the regions where the

evader will be captured by one pursuer and where the evader will be in minimum time cooperatively captured by both pursuers, thus providing the solution of the Game of Kind. This will differ from the point capture case and allow us to provide full state solutions for games with parameters that were previously not able to be solved, because of the lack of a closed SR. The algorithm for the construction of the players' optimal state feedback strategies in the state space region where both pursuer isochronously capture the evader is presented, thus providing the solution of the Game of Degree.

We will then move this focus into analyzing a similar differential game, this one derived from an Attacker-Defender-Target game. In it, we will again apply a radius of capture to our pursuer, but we will reduce his speed such that he will be slower than the evader. We will then determine the region in which the evader could reach while still avoiding the evader, determining what the locus of point in which he could not reach a target should the target be located at those points.

This paper is motivated by Air-to-Air Concept Operations. This research is useful in devising strategies for air-to-air combat and in autonomous decision making. We will determine the necessary conditions that would be required for an aircraft to ensure pursuit and capture of a potential aircraft.

The paper is organized as follows. The geometry of the basic Apollonius circle is discussed in Section 3.1, followed by the construction of Apollonius ovals in Sections 3.2 and 3.3. We introduce in Section 3.5 metrics for gauging the geometry of Apollonius ovals. The characterization of the Apollonius "oval" when the evader is faster than the pursuer is discussed in Sections 3.6 and 3.7. The Two Cutters and Fugitive Ship differential game is recast in a reduced state space whose dimension is three in Section 3.8. The solution of the Game of Kind and of the Game of Degree in the reduced state space is presented in Sections 4.1 and 4.2, respectively, followed

by examples in Section 4.6.

II. Background

This paper derives its concepts from two main sources. The first is game theory in its application of interactions between intelligent decision makers. The second is optimal control in its application of deriving the minimum time solution for capture. We will utilize game theory to devise and model the scenario that we are attempting to solve.

Game theory was originally developed by John von Neumann in 1928. It was defined in 1991 as "the study of mathematical models of conflict and cooperation between intelligent rational decision makers." This field of study has a broad range of applications from politics to economics. These games can vary in their objective, and can have two players cooperatively trying to obtain a cooperative objective or two players trying to achieve objectives that are antithetical to the other. We will deal with the latter case in the following discussion.

This paper deals with a subset of game theory where the dynamics are modeled using differential equations, as in control theory, called a differential game. The concept of a differential game was developed by Rufus Issacs in 1951, while he was working for the Rand Corporation. [1] We can use differential games to find solutions to real world scenarios in which we have multiple players attempting to reach a joint goal. In Isaacs' novel book, he gives several examples of types of differential games, where the players have various goals and changing parameters. One example of one of these differential games is the Homicidal Chauffeur differential game, described in Issacs [1] and Merz [3]. In this game, you have a purser and an evader, with the pursuer having a turning radius and attempting to capture the evader. In [3], the feedback strategies for this game are developed. This game provided a basis for a typical solution method for differential games; however, we will focus on a different type of game.

Our second source we derive this work from is the work done on optimal control. Much of optimal control was developed by Lev Pontryagin [4] and Richard Bellman [5]. They founded methods to solve optimal control problems in minimum time situations. This work led us to be able to solve for minimum time problems. We will utilize this work to devise solutions to our differential games as minimum time problems.

We wish to expand this work to include multiple agents. We want to study the two on one and many on one types of games. We have seen solutions to some types of two on one games and their applications in many fields, including that of air defense. [6], [7] Previous solutions to two on one games have focused on point capture [8], but we will be also focusing on finite capture sets. While this type of scenario isn't novel [9], we will be expanding these solutions for a fixed capture radius to determine the actual region of capture. The many on one game manifests itself generally in the form of a pursuer-evader-defender game. Again, these games have focused on the point capture problem, [10], while we will be focusing on finite radius of capture scenarios.

These types of games have shown to have direct application in air-to-air warfare. [11], [12] This research could be adapted to air combat in a more realistic scenario than the solutions that have been proposed so far for this type of engagement. This would be particularly useful in the case of missile defense, where the desired outcome would be to have an aircraft outside of a certain range of an exploding missile.

III. Methodology

3.1 Geometry

Isaacs' geometric solution of the "Two Cutters and the Fugitive Ship" game used the Apollonius circle geometric construct. The Apollonius circle is the locus in the Euclidean plane such that the ratio of distances to two fixed points, the foci, is constant — see Fig 1; in the context of our game, the foci of the Apollonius circle are the instantaneous positions of P and E. Let d be the P-E separation. The radius, ρ, of the Apollonius circle is

$$\rho = \frac{\mu}{1-\mu^2} d \tag{1}$$

and in an (x, y) Cartesian frame with E at the origin, its center O is at

$$x_O = \frac{\mu^2}{1-\mu^2} d, \quad y_O = 0 \tag{2}$$

The point I on the circumference of the Apollonius circle shown in Fig. 1 is where P will intercept a course holding E.

We may specify the Apollonius circle using polar coordinates as well. As seen in Fig 2, applying the law of cosines to ΔIPE we have:

$$\frac{1}{\mu^2} R^2 = d^2 + R^2 + 2Rd\cos(\theta)$$

which yields the quadratic equation in R

$$(\frac{1}{\mu^2} - 1)R^2 - d^2 - 2Rd\cos\theta = 0$$

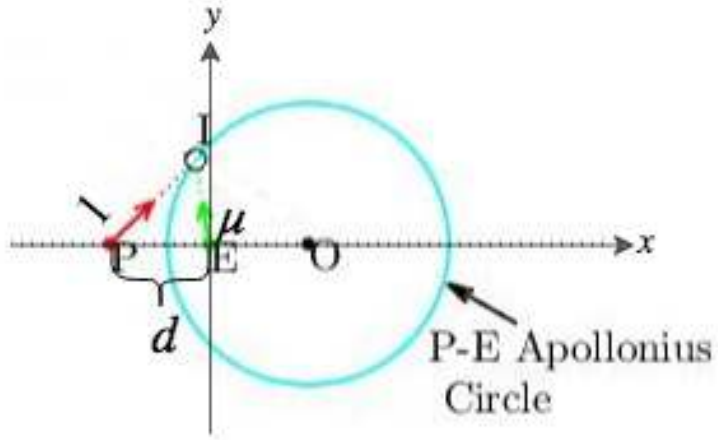

Figure 1: Apollonius Circle

Hence, in polar coordinates the Apollonius circle equation is

$$R(\theta) = \frac{\mu}{1-\mu^2}\left(\mu\cos\theta + \sqrt{1-\mu^2\sin^2\theta}\right)d\ , \quad \forall\ \theta \in [0, 2\pi] \tag{3}$$

The polar coordinate representation will be useful when the pursuer is endowed with a capture circle of radius $l > 0$ whereupon the SR is an Apollonius oval.

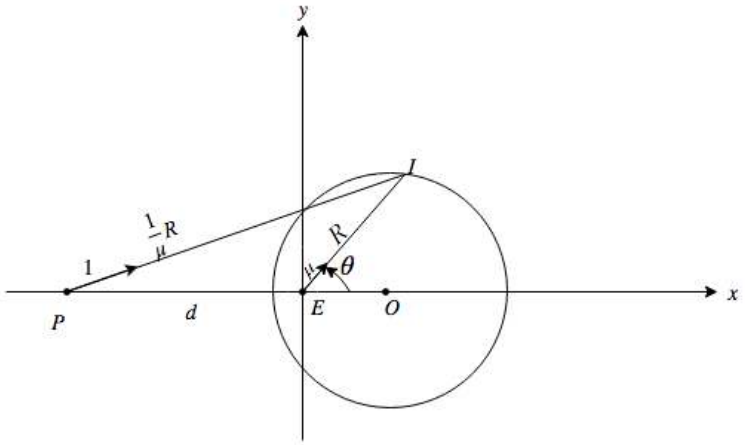

Figure 2: Apollonius Circle — Polar Coordinates

Since in the "Two Cutters and Fugitive Ship" pursuit-evasion differential game [1], [2] two pursuers are at work, we have an Apollonius circle/oval for each one of

the pursuers, say P_1 and P_2. The foci of the Apollonius circle C_1 are P_1 and E and the foci of the Apollonius circle C_2 are P_2 and E. Isaacs used this concept to find a geometrical solution to the differential game: The two Apollonius circles intersect at two points. The pursuers will isochronously and cooperatively capture the evader at the point of intersection of their respective Apollonius circles, at the point of intersection which is farther from E. It might also happen that the Apollonius circles don't intersect, that is, the small Apollonius circle is inside the bigger Apollonius disk. This signals that the evader will be single-handedly captured by one pursuer in Pure Pursuit (PP). The pursuer associated with the smaller Apollonius circle can always capture the Evader prior to the farther pursuer, and his optimal strategy is PP. This will also be the case if the Apollonius circles intersect but the point antipodal to E on the circumference of one of the Apollonius circles is inside the second Apollonius disk.

3.2 Apollonius Oval Construction

When the pursuer are endowed with a capture circle of radius $l > 0$, the Apollonius "circles" are Cartesian ovals. We shall refer to these as Apollonius ovals. We will develop a parametric representation to characterize the Apollonius ovals with a view to constructing the evader's Safe Region(SR) and the Boundary of the Safe Region (BSR). To construct the Apollonius oval when the capture radius $l > 0$, we start with the elementary pursuit-evasion game that has only two players, a pursuer and an evader, where the pursuer is endowed with a radius of capture $l > 0$. This is to say that if the distance between the pursuer and the evader is less than l, the evader will be captured. To justify our construction of the novel Apollonius ovals, we invoke the following

Lemma 1. *The Pursuer is endowed with a capture circle of radius l and he strives to*

capture the Evader in minimum time. Assume the Evader is obliged to pre-announce his course and to hold course. The Pursuer will employ Collision Course (CC) guidance and set his course s.t. the three points P, P', and E' are collinear, as shown in Figure 3. The optimal course of the Pursuer is determined upon solving the interception triangle $\Delta E'PE$. A solution exists irrespective of the course chosen by the Evader, provided the speed ratio $\mu \triangleq \frac{V_E}{V_P} < 1$.

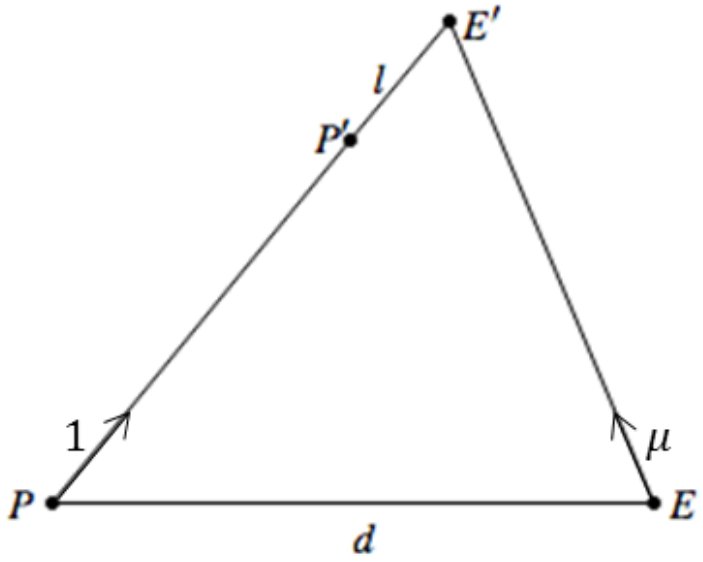

Figure 3: Interception Triangle

Proof. Suppose the optimal solution is s.t. the path P, P', E' is kinked — see Figure 4. Consider the circular arc of radius $\overline{PP'}$ centered at P and the straight line $\overline{PE'}$. Let P^* be the point where the circular arc intersects the straight line $\overline{PE'}$. By construction, $\overline{PP^*} = \overline{PP'}$, but the triangle inequality yields

$$\overline{PP^*} + \overline{P^*E'} \leq \overline{PP'} + l$$

so

$$\overline{P^*E'} \leq l$$

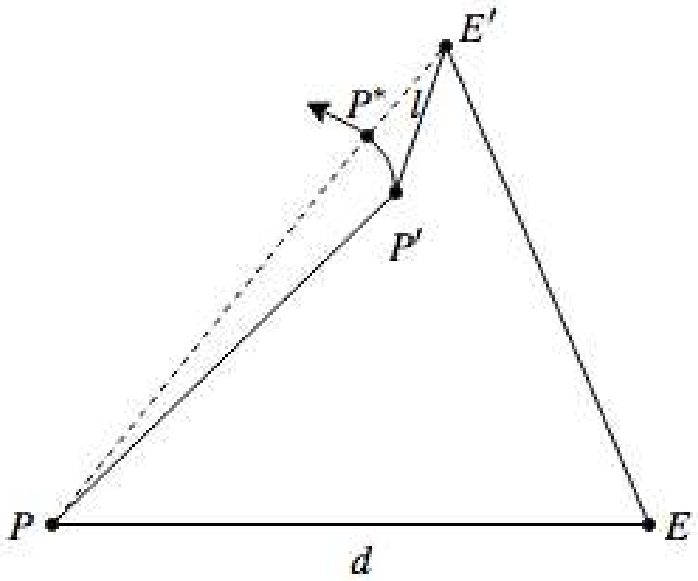

Figure 4: Non-Optimal Configuration

Hence, choosing the path PP^* which takes as long as the path PP' would have caused the Pursuer to overshoot the target/Evader. Hence, the path PP' is not optimal – the triangle inequality must be an equality, that is, the three points P, P', E' must be collinear. □

3.3 Parameterization of Apollonius Ovals

If the Evader starts at the (x, y) plane's origin with speed $\mu < 1$ and, without loss of generality, a pursuer with speed 1 starts at $(-d, 0)$, as seen in Figure 5, then we have the following two equations which allow us to determine the elemental BSR for the evader, that is, the E, P Apollonius oval:

$$\mu^2 t^2 = x^2 + y^2 \tag{4}$$

$$(t + l)^2 = (x + d)^2 + y^2 \tag{5}$$

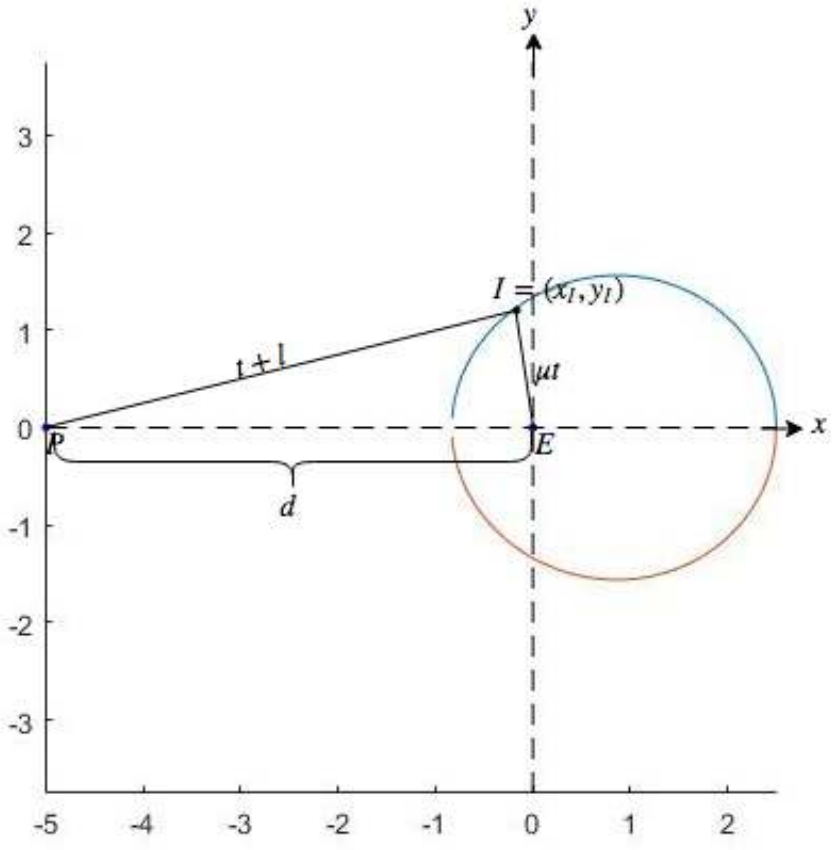

Figure 5: Apollonius Oval

We subtract Equation (4) from Equation (5) and, upon solving a quadratic equation, obtain the equation of the Apollonius oval in parametric form

$$\begin{aligned} x(t) &= \frac{(1-\mu^2)t^2 + 2lt + l^2 - d^2}{2d} \\ y(t) &= \sqrt{\mu^2 t^2 - \frac{[(1-\mu^2)t^2 + 2lt + l^2 - d^2]^2}{4d^2}} \quad , \quad -\frac{d+l}{1+\mu} \leq t \leq \frac{d-l}{1-\mu} \end{aligned} \tag{6}$$

Equation (6) specify the Apollonius oval in parametric form. The minimum and maximum values for x are realized in head on and tail chase encounters,

$$-\frac{\mu}{1+\mu}(d-l) \leq x \leq \frac{\mu}{1-\mu}(d-l) \tag{7}$$

and to find the maximum y-coordinate, or height, of the Apollonius oval, we will take

the derivative of the function $y(t)$ and set it equal to 0. The equation that determines the value of t for which y is maximized is the cubic

$$(1-\mu^2)^2t^3 + 2l(1-\mu^2)t^2 + [2l^2 + \mu^2l^2 - \mu^2d^2 - d^2]t + l(l^2 - d^2) = 0 \qquad (8)$$

which has a real positive root $t > 0$. When $0 < l << d$, the cubic has three real roots and the maximal root determines y_{max}. When this value of t is substituted into Equation (6), we obtain y_{max}.

3.4 Equal Speed Geometry

We will now look at the geometry of the special case where the three players have equal speeds. The Two Cutters and Fugitive Ship differential game is solved using a geometric method — no HJBI PDE here. The validity of the geometric method was proved in [2]. When a pursuer and an evader; both with simple motion á la Isaacs, have the same speed and the pursuer is endowed with a radius of capture l, the locus of points in the Euclidean plane which they can reach at the same time is a hyperbola. Therefore, for any value of capture range $l > 0$ of the pursuers, what would have been an Apollonius oval had the pursuer been faster than the evader [13] will become a hyperbola and the Boundary of the Safe Region of the Evader (BSR) will be delineated by an arc of the hyperbola

$$\frac{x^2}{a^2} - \frac{y^2}{b^2} = 1$$

with the parameters

$$a = \frac{l}{2}\ , \quad b = \frac{1}{2}\sqrt{d^2 - l^2}$$

where d is the $P-E$ separation. Since there are two pursuers, there are two hyperbolae at play. We will use the asymptotes of those hyperbolae to solve the Game of Kind,

and these are given by

$$y = \pm \frac{b}{a} x$$

It will be useful to define the hyperbola's "eccentricity" $e \triangleq \frac{d}{l}$, and so the asympototes' slope is

$$\frac{b}{a} = \sqrt{e^2 - 1} \tag{9}$$

The hyperbola locus, whose foci are the instantaneous positions of the pursuer P and the Evader E, and it's asymptotes, are shown in Figure 6. We use the hyperbola construct to designate the Safe Region (SR) of E in the Two Cutters and Fugitive Ship differential game. Figure 6 shows the Boundary of the Safe Region (BSR) in the realistic plane when the pursuer is at $(-\frac{d}{2}, 0)$ and the evader at $(\frac{d}{2}, 0)$. Because the Pursuer is not faster than the Evader, this BSR is open; in other words, the Evader can escape. Hence, we need at least one other pursuer to obtain a closed SR.

In the version of the Two Cutters and Fugitive Ship Differential Game investigated herein we have two pursers with capture radius l and one evader, with all three having the same speed. We use a rotating reference frame (x, y), with the x-axis running through the instantaneous positions of the Pursuers P_1 and P_2 and the y-axis is the orthogonal bisector of the segment $\overline{P_1 P_2}$. The state is specified by three variables: half of the separation of the pursuers, x_p, and the x and y position of the evader, (x_E, y_E). For example, the symmetric situation E, P_1, and P_2 are collinear and the Evader is located halfway between P_1 and P_2 is illustrated in Figure 7. This figure shows both the hyperbolae and their asymptotes, which intersect. The SR is bounded.

There are three important points labeled in Figure 7: I, I', and I''. I' and I'' are the points of intersection of the asymptotes. The existence of these points provides the solution to the Game of Kind. If the asympototes don't intersect the evader can escape capture. If the hyperbolae intersect and E is in the lends shaped region formed

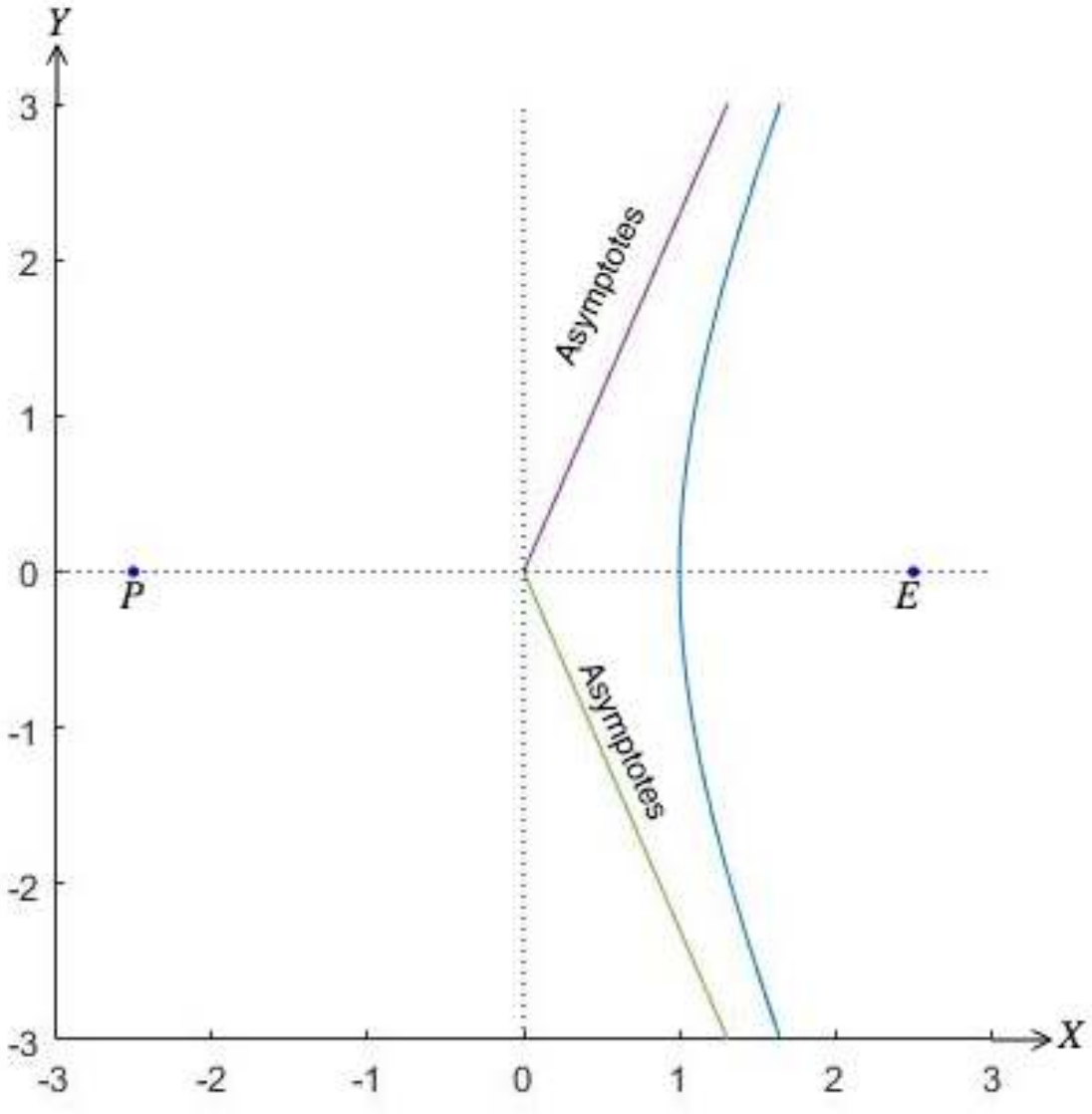

Figure 6: The Hyperbola is the BSR of E

by the intersecting hyperbolae, if the pursuers play optimally, captures of the Evader is guaranteed. I_1 and I_2 are the points of intersection of the (P_1, E) and (P_2, E) based hyperbolae. Each of these points will be important in the next two sections. Our goal is to determine whether the SR is bounded, which obviously is the case in the symmetric configuration illustrated in Figure 7, where the evader is hemmed in by the pursuers and the asymptotes of the hyperbolae intersect.

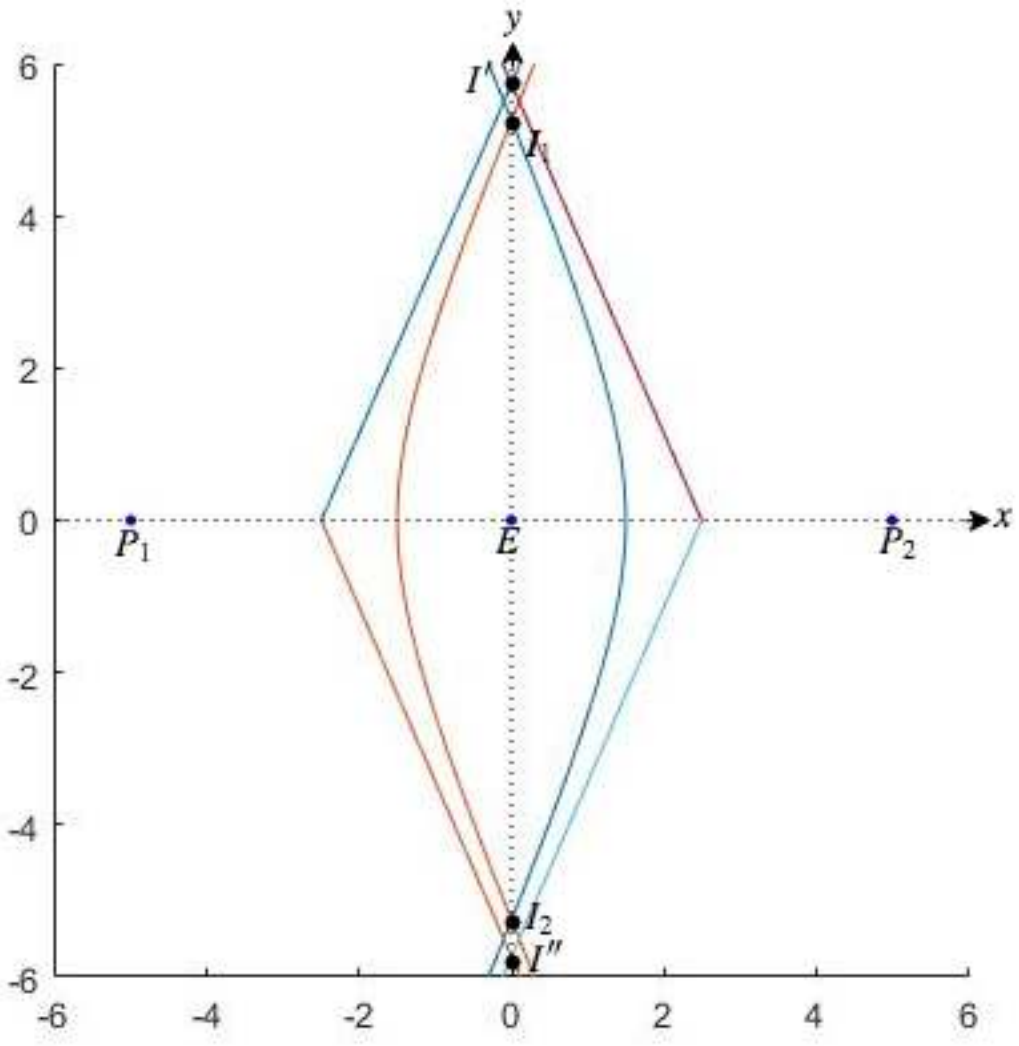

Figure 7: Two Pursuer Action

3.5 Metrics

To gauge the Apollonius oval's dependence on the speed ratio μ and the ratio of the radius of capture l to the initial distance d between P and E, we introduce the following three metrics: eccentricity, e, and two definitions of the Apollonius oval's Aspect Ratio, $Æ_1$ and $Æ_2$. The three metrics are defined as follows.

$$e = \sqrt{1 - \frac{b^2}{a^2}} \tag{10}$$

$$\text{Æ}_1 \equiv \frac{a}{b} \tag{11}$$

$$\text{Æ}_2 \equiv \frac{a}{y(x=0)} \tag{12}$$

where b is the length of the "semi-minor" axis and a is the length of the "semi-major" axis of the Apollonius oval. Here,

$$a \equiv \frac{1}{2}(x_{\max} - x_{\min}) \ , \qquad b \equiv y_{\max}$$

and $x_{\min}$, $x_{\max}$, $y_{\max}$ are shown in Figure 8 where an Apollonius oval with $\mu = \frac{1}{2}$ and $\frac{d}{l} = 2$ is illustrated: $x_{\min} = -\frac{5}{6}$, $x_{\max} = \frac{5}{2}$, $y_{\max} = 1.561$, $e = .123$, $\text{Æ}_1 = 1.068$, $\text{Æ}_2 = 1.25$. Note however that the Apollonius ovals are not ellipses.

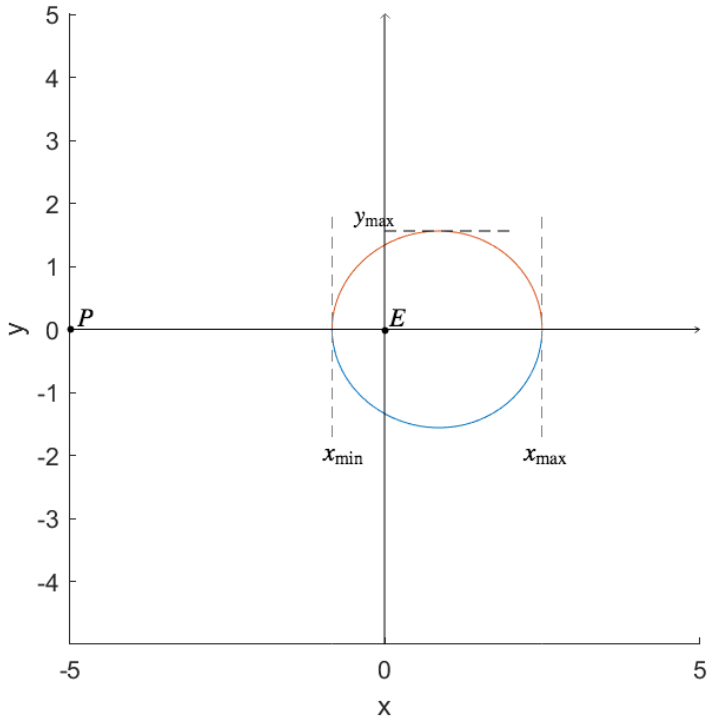

Figure 8: Apollonius Oval: $\mu = \frac{1}{2}$, $\frac{d}{l} = 2$

We investigate how these Apollonius ovals' metrics are dependent on the speed ratio parameter μ and the ratio of the distance d between the pursuer and evader and the radius of capture l: In the classical case, when $l = 0$, these Apollonius circle's metrics are $e = 0$ and $Æ_1 = Æ_2 = 1$.

To quantify how the Apollonius oval changes as the problem parameters μ or $\frac{l}{d}$ vary, we use the eccentricity (e) and Aspect Ratio ($Æ$) metrics (10)-(12). To this end, we use the parametric equations above to first calculate the values for a and b, the respective length and the width of the Apollonius oval.

$$a = \frac{\mu}{1-\mu^2}(d-l)\ , \qquad b = \sqrt{\mu^2\bar{t}^2 - \frac{[(1-\mu^2)\bar{t}^2 + 2l\bar{t} + l^2 - d^2]^2}{4d^2}}\ ,$$

where $\bar{t}$ is the maximal real positive root of the cubic Equation (8).

In the limiting case, when the speed ratio $\mu = 1$, the BSR is a hyperbola and the aspect ratios

$$Æ_1 = \frac{\frac{l}{d}}{\sqrt{1-(\frac{l}{d})^2}}$$

$$Æ_2 = \frac{1-\frac{l}{d}}{\sqrt{1-\mu^2(1-(\frac{l}{d})^2)}-\frac{l}{d}}$$

The evader is slower than the pursuer, so E is always located inside the Apollonius ovals — see Fig. 9. When we evaluate this for $\mu = 1$, we obtain the envelope of the family of Apollonius ovals parameterized by $0 < \mu < 1$. It is the hyperbola

$$\frac{(x+\frac{d}{2})^2}{a^2} - \frac{y^2}{b^2} = 1 \tag{13}$$

where

$$a = \frac{l}{2}\ , \quad b = \frac{1}{2}\sqrt{d^2-l^2},$$

as shown Figure 9.

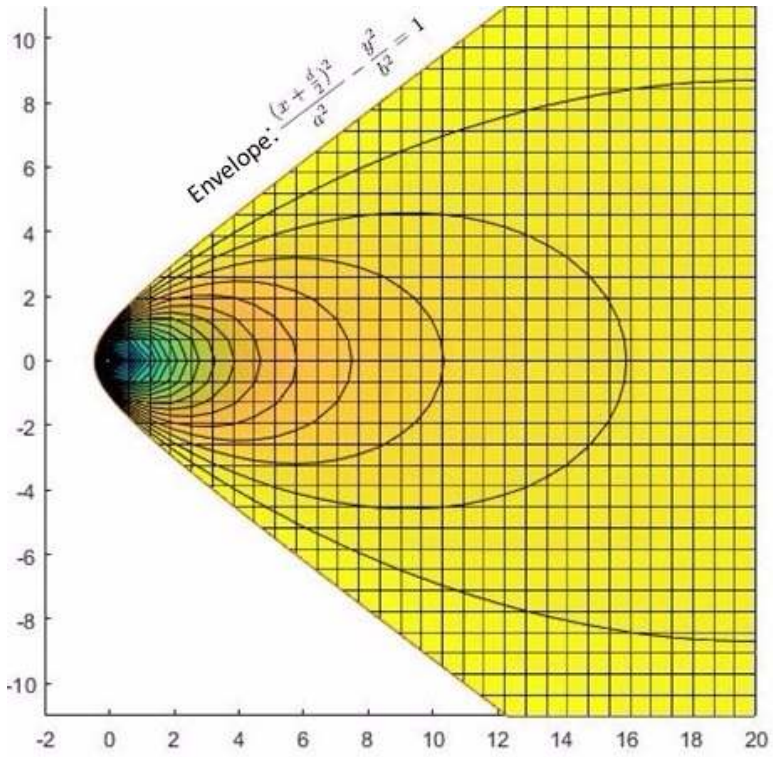

Figure 9: Family of Apollonius ovals, $0 \leq \mu \leq 1$, $\frac{l}{d} = .8$

The dependence of the eccentricity e of the Apollonius ovals on the parameters μ and l is shown in Figure 10. The Apollonius ovals' eccentricity increases as the P-E separation d approaches l. In Figures (10) and (11) we show the dependence on l of the 3 metrics: eccentricity and the two $\acute{A}$Rs, as a function of the ratio $\frac{l}{d}$. These graphs confirm the earlier derived results.

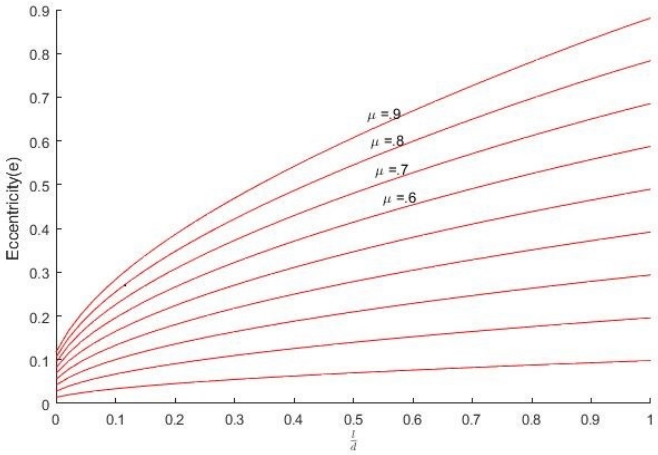

Figure 10: Eccentricity of Apollonius Ovals

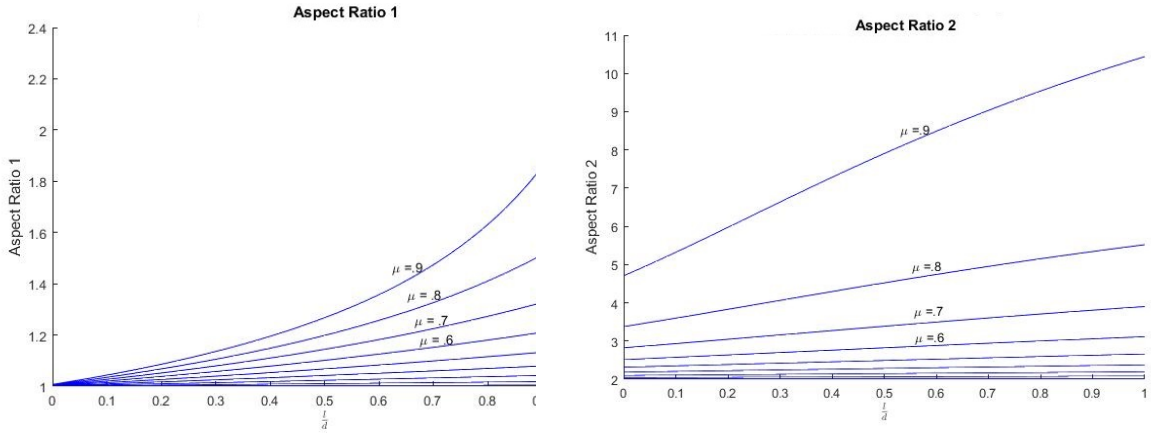

Figure 11: Apollonius Oval's Aspect Ratio dependence on the parameters μ and $\frac{l}{d}$

3.6 Slower Pursuer — Point Capture

Restructuring this for the case where the pursuer is slower than the evader and now redefining the speed ratio $\frac{v_E}{v_P} = \frac{1}{\mu}$ so that $\mu \leq 1$, we derive the equation for the Apollonius circle as follows — see Fig 12, where now the origin is collocated with the Pursuer P. We apply the law of cosines to ΔIEP which gives

$$R^2 = \frac{1}{\mu^2}R^2 + d^2 - 2\frac{1}{\mu}Rd\cos\varphi$$

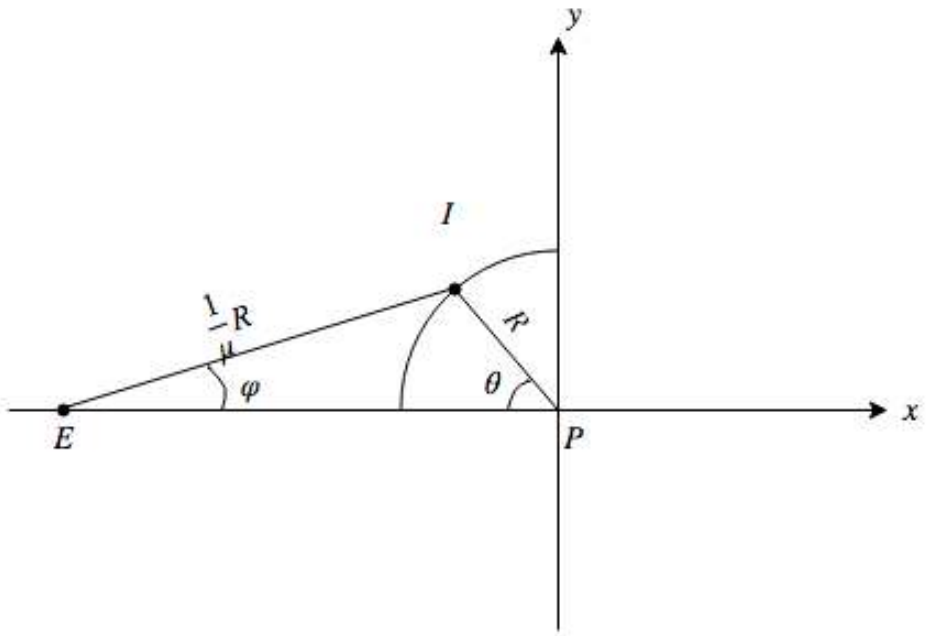

Figure 12: Apollonius Circle — Slow Pursuer

This is a quadratic equation in R,

$$(\frac{1}{\mu^2} - 1)R^2 + d^2 - 2\frac{1}{\mu}Rd\cos\varphi = 0$$

To have a real solution, the evader's course must satisfy

$$0 \leq \varphi \leq A\sin\mu \tag{14}$$

and the Apollonius circle is

$$R(\varphi) = \frac{\mu}{1-\mu^2}\left(cos\varphi - \sqrt{\mu^2 - \sin^2\varphi}\right)d \ , \quad \forall\ \varphi \in [0, A\sin\mu] \tag{15}$$

When $\varphi = A\sin\mu$, the radial from E is tangent to the Apollonius circle arc's endpoint which is at $(0, \frac{\mu}{\sqrt{1-\mu^2}}d)$.

Next we apply the law of sines to ΔIEP which gives

$$\sin\theta = \frac{1}{\mu}\sin\varphi \ , \quad 0 \leq \theta \leq \frac{\pi}{2}$$

and so, in polar coordinates the Apollonius oval arc when the evader is faster than the pursuer is

$$R(\theta) = \frac{\mu}{1-\mu^2}\left(\sqrt{1-\mu^2\sin^2\theta} - \mu\cos\theta\right)d \ , \quad \forall\ \theta \in [0, \frac{\pi}{2}] \tag{16}$$

The second solution of the quadratic equation is

$$R(\varphi) = \frac{\mu}{1-\mu^2}\left(\cos\varphi + \sqrt{\mu^2 - \sin^2\varphi}\right)d \ , \quad \forall\ \varphi \in [0, A\sin\mu]$$

Hence, using the parameter θ,

$$R(\theta) = \frac{\mu}{1-\mu^2}\left(\sqrt{1-\mu^2\sin^2\theta} + \mu\cos\theta\right)d \ , \quad \forall\ \theta \in [\frac{\pi}{2}, \pi] \tag{17}$$

So now, when the evader is faster than the pursuer the complete Apollonius circle in polar coordinates is given by Equations (16) and (17).

We have formally obtained the Apollonius circle, however only its "leading edge" arc which is delineated by the point of tangency to the Apollonius circle of the $\overline{EI}$ segment is relevant as far as the differential game is concerned. Therefore, returning to Equation (15), the maximum φ value is given using Equation 14. Indeed, when E is faster than P the Usable Part of the Apollonius circle is the arc given by Equation 15.

3.7 Slower Pursuer — Apollonius "Oval" Parametrization

When $l > 0$, we use Fig 13 and the law of cosines to find the maximum value

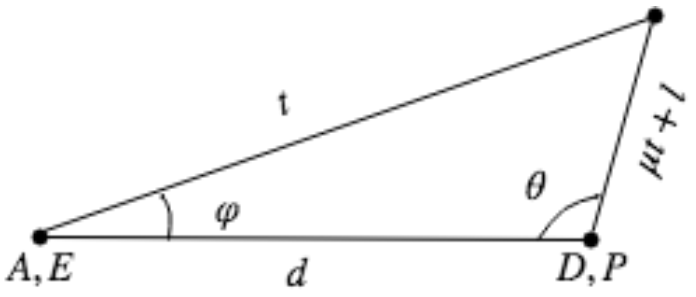

Figure 13: Capture with Finite Capture Radius $l > 0$

$$d^2 + t^2 - 2dt\cos\varphi = (\mu t + l)^2$$

so,

$$(1-\mu^2)t^2 - 2t(d\cos\varphi + \mu l) + d^2 - l^2 = 0 \ , \quad \forall\ \varphi \in [0, \varphi_{\max}]$$

we then find that

$$(d\cos\varphi_{\max} + \mu l)^2 - (1-\mu^2)(d^2 - l^2) = 0$$

which leads to

$$\cos\varphi_{\max} = \sqrt{1-\mu^2}\sqrt{1-(\frac{l}{d})^2} - \mu\frac{l}{d}$$

The scenario when the evader is faster than the pursuer is relevant to the differential game of guarding a target, where the Attacker (A), here represented by E, is trying to avoid a slower Defender (D), here represented by P, while striving to reach a target set in $\mathbb{R}^2$. The Apollonius oval then helps delineate the region where the defender will be able to reach the target before the attacker. Should $E(A)$ pre-announce his course, he will be intercepted by $P(D)$ provided his course $0 \le \varphi \le \cos\varphi_{\max}$; if $\varphi > A\sin\mu$, $P(D)$ cannot touch $E(A)$.

It is interesting to also consider Apollonius ovals in the case of a faster evader, that

is, μ is redefined as $\mu = \frac{v_P}{v_E} \leq 1$. To this end, we will also redefine the objective for the players. In this model, the desire of the purser will be to capture the evader. The evader's objective is defined in this case to be to reach points beyond the pursuer. In Figure 5, the position of the Evader and Pursuer are interchanged. The Evader's SR in this case is obviously not bounded. Figure 14 indicates how this Apollonius oval is constructed: P is now in the interior of the Apollonius oval and the following holds,

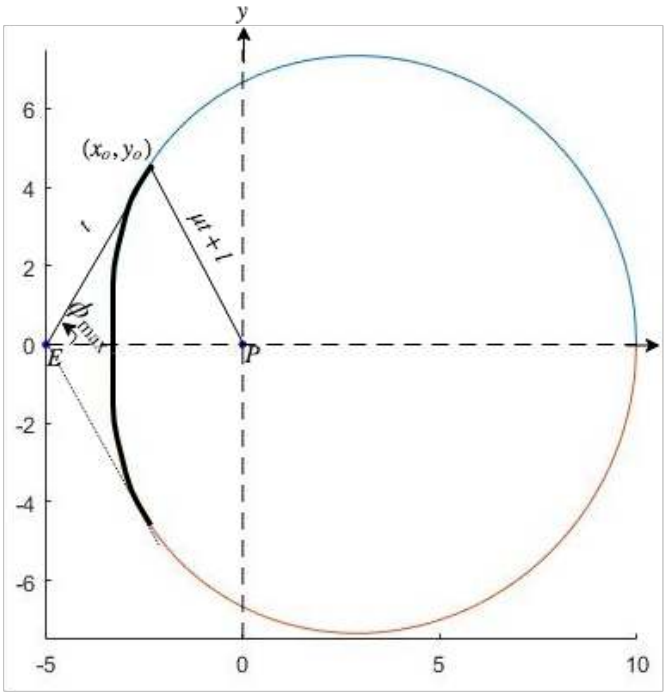

Figure 14: Apollonius "Oval" when Evader is Faster than the Pursuer; $\frac{l}{d} = 0.8$, $\mu = 0.5$

$$(\mu t + l)^2 = x^2 + y^2 \tag{18}$$

$$t^2 = (x + d)^2 + y^2 \tag{19}$$

This yields the parametric representation of the Apollonius oval

$$x(t) = \frac{(1 - \mu^2)t^2 - 2\mu l t - l^2 - d^2}{2d} \tag{20}$$

$$y(t) = \sqrt{t^2 - \frac{[(1-\mu^2)t^2 - 2\mu l t - l^2 + d^2]^2}{4d^2}} \quad , \quad \frac{d-l}{1+\mu} \leq t \leq \frac{d+l}{1-\mu} \tag{21}$$

Similar to the slower Evader case, the x limits come from the head on and tail chase "encounters":

$$-\frac{\mu d + l}{1+\mu} \leq x \leq \frac{d+l}{1-\mu} \tag{22}$$

Additionally, we have at $x = 0$,

$$y = \frac{\mu\sqrt{(1-\mu^2)d^2 + l^2} + l}{1-\mu^2} \tag{23}$$

This Apollonius oval has a qualitatively different shape than in the conventional, slower evader, case. In the slower pursuer case, we plot the Apollonius oval which is given in parametric form in Equations (20) and (21), and the result is shown in Figure (15). The Apollonius oval is dented on the x-axis when the pursuer's capture radius l increases, and when d increases, the Apollonius oval expands. In Figure 15, we see a dented "oval" when $\frac{l}{d} = 1$.

We have formally obtained the Apollonius oval however its "leading edge" which is delineated by the points of tangency to the Apollonius oval of the two straight lines emanating from E is relevant to the differential game under consideration. We can then see calculate the new bounds for t by calculating the value at $\varphi_{\max}$. This gives us

$$t_{\max} = \sqrt{\frac{d^2 - l^2}{1-\mu^2}}$$

This gives us a curve which delineate a barrier in which the evader cannot cross without being captured. Because this region is open, it does not provide a full BSR for the evader.

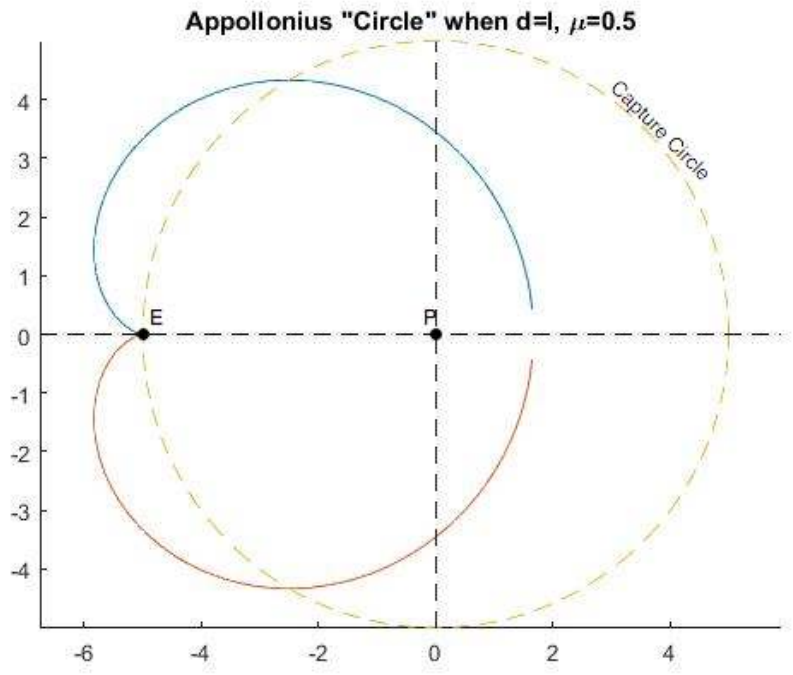

Figure 15: Apollonius Oval for Slower Pursuer and $d = l$, No Usable Part

3.8 Reduced State Space

The "Two Cutters and the Fugitive Ship" differential game has six states. Isaacs solved the "Two Cutters and Fugitive Ship" differential game in the realistic plane. It is however beneficial to analyze our differential game in a reduced state space, similar to Isaacs' treatment of the Homicidal Chauffeur differential game [1]. The dimension of our game's state space can be reduced to three using a non-inertial, rotating reference frame, by pegging the x-axis to the instantaneous positions of P_1 and P_2. The y-axis is the orthogonal bisector of the $\overline{P_1P_2}$ segment. In this rotating (x, y) reference frame the states are E's x and y-coordinates (x_E, y_E) and the x - position x_P of P_1; the position of P_2 is $(-x_P, 0)$ Thus, if in the realistic plane (X, Y) the positions of the players are $P_1 = (X_{P_1}, Y_{P_1})$, $P_2 = (X_{P_2}, Y_{P_2})$, $E = (X_E, Y_E)$, in the reduced state space

$$x_P = \frac{1}{2}\sqrt{(X_{P_1} - X_{P_2})^2 + (Y_{P_1} - Y_{P_2})^2 x}$$

$$x_E = \frac{(X_E - \frac{1}{2}X_{P_1} - \frac{1}{2}X_{P_2})(X_{P_2} - X_{P_1}) + (Y_E - \frac{1}{2}Y_{P_1} - \frac{1}{2}Y_{P_2})(Y_{P_2} - Y_{P_1})}{\sqrt{(X_{P_1} - X_{P_2})^2 + (Y_{P_1} - Y_{P_2})^2}}$$

$$y_E = \frac{-(X_E - \frac{1}{2}X_{P_1} - \frac{1}{2}X_{P_2})(Y_{P_2} - Y_{P_1}) + (Y_E - \frac{1}{2}Y_{P_1} - \frac{1}{2}Y_{P_2})(X_{P_2} - X_{P_1})}{\sqrt{(X_{P_1} - X_{P_2})^2 + (Y_{P_1} - Y_{P_2})^2}}$$

In this reduced state space the y-coordinates of P_1 and P_2 will be 0, the position of P_1 will always be $(x_P, 0)$ and the position of P_2 will always be $(-x_P, 0)$. Without loss of generality we assume $x_E \geq 0$ and $y_E \geq 0$. The rotating reference frame (x,y) is shown overlaid on the realistic plane (X,Y) in Figure 16 where the P_1, E and P_2 players' respective headings χ, ϕ and ψ are also indicated. The player's headings in the realistic plane and in the reduced state space are related according to

$$\psi = \psi + \theta \ , \quad \chi = \chi + \theta \ , \quad \phi = \phi + \theta$$

where

$$\sin\theta = \frac{Y_{P_2} - Y_{P_1}}{2x_P} \ , \quad \cos\theta = \frac{X_{P_2} - X_{P_1}}{2x_P}$$

Without loss of generality, the rotating reference frame (x, y) is initially aligned with the inertial frame (X, Y).

Using the rotating reference frame (x,y), the state space of the Two Cutters and Fugitive Ship differential game is reduced to the first quadrant of R^3, that is, the set

$$R_1^3 \equiv \{(x_P, x_E, y_E) \mid x_P \geq 0, y_E \geq 0\}$$

and symmetry allows us to confine our attention to the case where $x_E \geq 0$ so, the

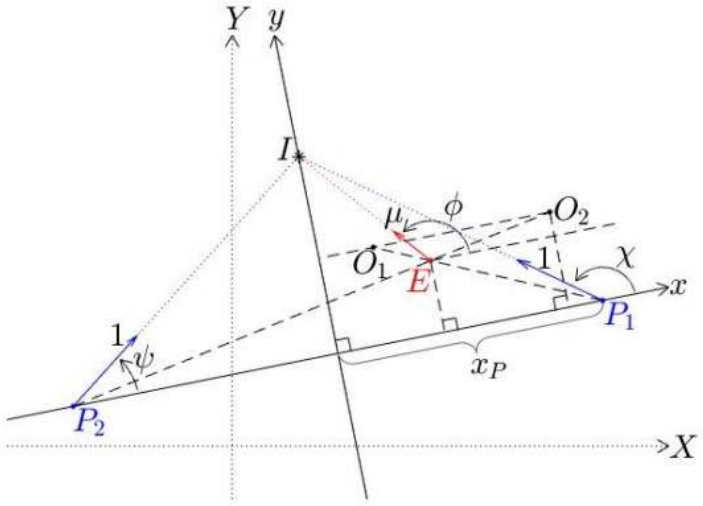

Figure 16: Rotating Reference Frame

state will evolve in the positive orthant of R^3, that is, in

$$R^3_+ = \{(x_P, x_E, y_E) \mid x_P \geq 0, x_E \geq 0, y_E \geq 0\}$$

The three-state nonlinear dynamics of the "Two Cutters and Fugitive Ship" differential game in the reduced state space now are

$$\dot{x}_P = \frac{1}{2}(\cos\chi - \cos\psi), \;\; x_P(0) = x_{P_0} \tag{24}$$

$$\dot{x}_E = \mu\cos\phi - \frac{1}{2}(\cos\chi + \cos\psi) + \frac{1}{2}\frac{y_E}{x_P}(\sin\chi - \sin\psi), \;\; x_E(0) = x_{E_0} \tag{25}$$

$$\dot{y}_E = \mu\sin\phi - \frac{1}{2}(\sin\chi + \sin\psi) - \frac{1}{2}\frac{x_E}{x_P}(\sin\chi - \sin\psi), \;\; y_E(0) = y_{E_0} \tag{26}$$

IV. Results & Analysis

4.1 Game of Kind

We concern ourselves with two Pursuers, each faster than the Evader, both endowed with a radius of capture $l > 0$.

We partition the game's state space into a region $R_{1,2}$ where both pursuers cooperatively and isochronously capture the Evader and into additional two regions, R_1 and R_2, where pursuer P_1 or pursuer P_2 single-handedly capture the evader in PP. We obtain the separating surfaces between R_1, R_2 and $R_{1,2}$ in the reduced state space: The regions in which the Evader will only be captured by one pursuer, P_1 or P_2 and the region where the evader will cooperatively be captured by both pursuers isochronously.

Let R_1 be the state space region where E is single-handedley captured by pursuer P_1, R_2 is the state space region where E is single-handedly captured by P_2 and $R_{1,2}$ is the state space region where E is isochronously captured by the cooperating pursuers P_1 and P_2. To find the surface in the reduced state space's positive orthant which separates R_1 and $R_{1,2}$, we look at the critical state at which capture by P_1 and P_2 occurs isochronously and at the same time E is captured by P_1 in PP. The geometry is illustrated in Fig. 17.

The critical situation arises when the point I, where E is captured in PP by P_1, is on the y-axis, for there E will also be captured by P_2. Let t be the time-to-capture at I. This gives us the following equations to find t, and subsequently the evader's

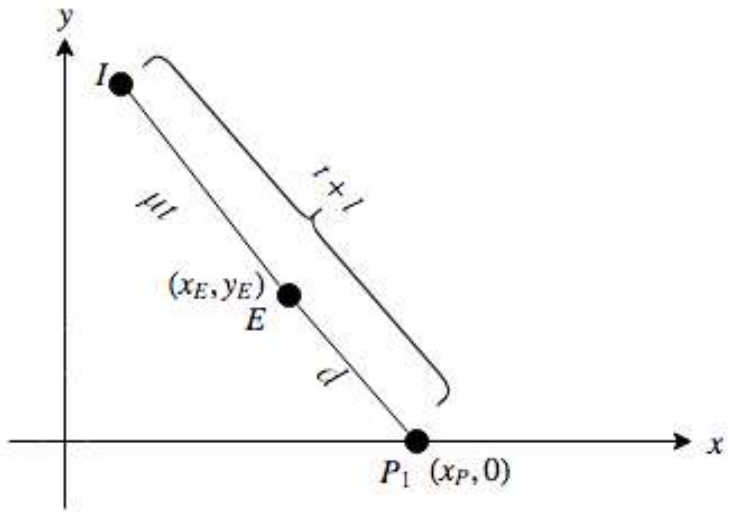

Figure 17: Critical Configuration

point of interception $I = (x_I, y_I)$:

$$\mu t + d = t + l$$

Hence

$$t = \frac{1}{\mu}(d - l)$$

At the same time

$$\overline{IP}_1 = d + \mu t$$

Substituting in the value for t, we obtain,

$$\overline{IP}_1 = \frac{1}{1-\mu}(d - l)$$

Because of similar triangles, we find:

$$\frac{x_P - x_I}{\frac{1}{1-\mu}(d-l)} = \frac{x_P - x_E}{d}$$

so

$$x_I = \frac{1}{1-\mu}\frac{1}{d}[\mu(l-d)x_P + (d-\mu l)x_E]$$

and

$$\frac{y_I}{\frac{1}{1-\mu}(d-l)} = \frac{y_E}{d} \ ,$$

we calculate

$$x_I = \frac{1}{1-\mu}\frac{1}{d}[(d-\mu l)y_E]$$

with

$$d = \sqrt{(x_P - x_E)^2 + y_E^2}$$

The Pursuer, the Evader, and the interception point I on the y-axis are collinear. The second pursuer in the LHP is also on the x-axis. The first pursuer and the Evader are initially a distance d apart, as is shown in Figures 17 and 18.

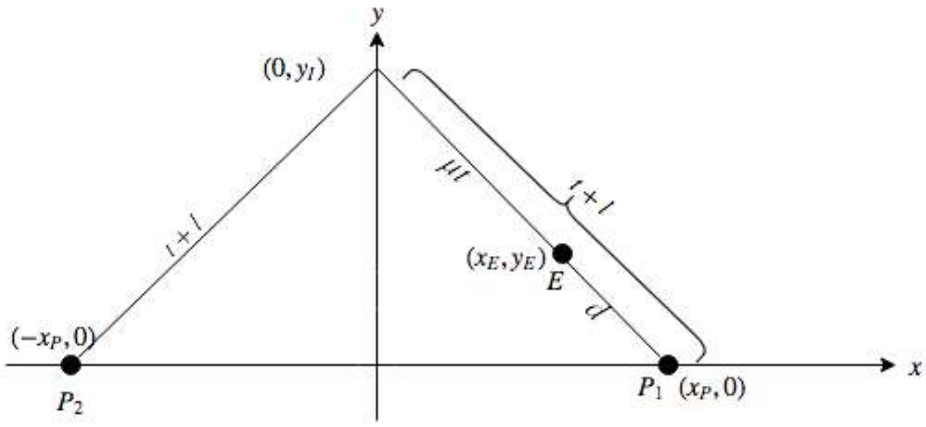

Figure 18: Critical Geometry

This gives

$$\mu(d-l)x_P = (d-\mu l)x_E$$

or

$$(\mu x_P - x_E)d = \mu l(x_P - x_E)$$

hence

$$d = \mu l \frac{x_P - x_E}{\mu x_P - x_E}$$

Next, in the right triangle with the hypotenuse of $\overline{P_1 E}$

$$(x_P - x_E)^2 + y_E^2 = d^2$$

Substituting in the expression for d and solving for y_E gives

$$y_E = \frac{x_P - x_E}{\mu x_P - x_E} \sqrt{\mu^2 l^2 - (\mu x_P - x_E)^2}$$

When $y_E = 0$, this gives the line $x_E = \mu x_P - \mu l$, as expected. Alternatively,

$$(d - \mu l) x_E \leq \mu (d - l) x_P$$

or,

$$\mu l (x_p - x_E) \leq d (\mu x_p - x_E)$$

When $y_E = 0$,

$$\mu l (x_P - x_E) \leq (x_P - x_E)(\mu x_P - x_E)$$

$$x_E \leq \mu x_P - \mu l$$

Hence, in the first orthant of the reduced state space (x_P, x_E, y_E) the surface separating the sets R_1 and $R_{1,2}$ is

$$y_E(x_P, x_E) = \frac{x_P - x_E}{\mu x_P - x_E} \sqrt{\mu^2 l^2 - (\mu x_P - x_E)^2} \ , \quad l + \frac{1}{\mu} x_E \geq x_P \geq \frac{1}{\mu} x_E \tag{27}$$

In the plane $x_E = 0$, we have the circular arc

$$y_E(x_P) = \sqrt{l^2 - x_P^2}\ , \quad 0 \geq x_P \geq l$$

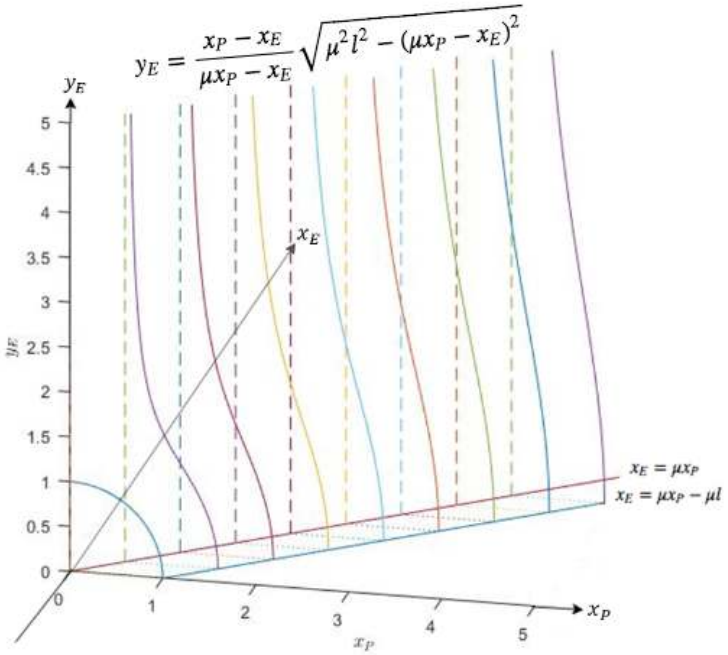

Figure 19: Solution of the Game of Kind; $l = 1$, $\mu = \frac{1}{2}$

In Figure 19 the state space region $R_{1,2}$ where E is isochronously captured by P_1 and P_2 is separated from the region where E is single-handedly captured by P_1 by the surface covered by the family of curves (27) which is parametrized by x_E. E is single-handedly captured by P_1 in the region included between this surface and the plane $x_P = 0$. The mirror image of Figure 19 about the plane $x_E = 0$ yields the region R_2 where E is single-handedly captured by P_2. The region $R_{1,2}$ where P_1 and P_2 cooperatively and isochronously capture E is symmetric about the plane $x_E = 0$. The surface separating the sets R_1, and $R_{1,2}$ shown in Figure 19 is parametrized by

μ and l. When $l = 0$, this is the wedge [2]:

$$R_{1,2} = \{(x_P, x_E, y_E) | x_P \geq 0, y_E \geq 0, -\mu x_P \leq x_E \leq \mu x_P\}$$

4.2 Game of Degree

The Apollonius ovals constructed in Sections 3.2 and 3.3 are used to obtain the solution in $R_{1,2}$ of the two-on-one pursuit-evasion Game of Degree. Similar to Isaacs' geometric method applied to the Two Cutters and Fugitive Ship scenario in [1], the players' optimal state feedback strategies are obtained upon calculating the intersection of the two Apollonius ovals C_1 and C_2 which pertain to pursuers P_1 and P_2, respectively. This yields the SR of E.

Using the Apollonius ovals construct, we obtain the geometric solution of the two-on-one pursuit-evasion game in $R_{1,2}$ by forming the composite, lens shaped, BSR of the Evader. The two Apollonius ovals are shown in Figure 20. The Apollonius ovals intersect at two points. The point of intersection of the two Apollonius ovals which is farther from E yields the players' aim point I. The evader and the two pursuers head to the aim point I where the evader will be isochronously captured by the two pursuers. Once the aim point I is calculated as a function of the current game's reduced state (x_P, x_E, y_E), the players' optimal state feedback strategies are obtained.

We analyze the Game of Degree in the three-dimensional reduced state space. In the rotating reference frame (x, y) the pursuers start at the points $(-x_P, 0)$ and $(x_P, 0)$ so a translation and a rotation transformation is required. We use the parametric representation of the Apollonius ovals in Equation (6) where they are given in an evader-centered reference frame (X, Y). The frame (X_1, Y_1) where the Apollonius oval C_1 resides is rotated relative to the (x, y) frame by an angle α and the frame

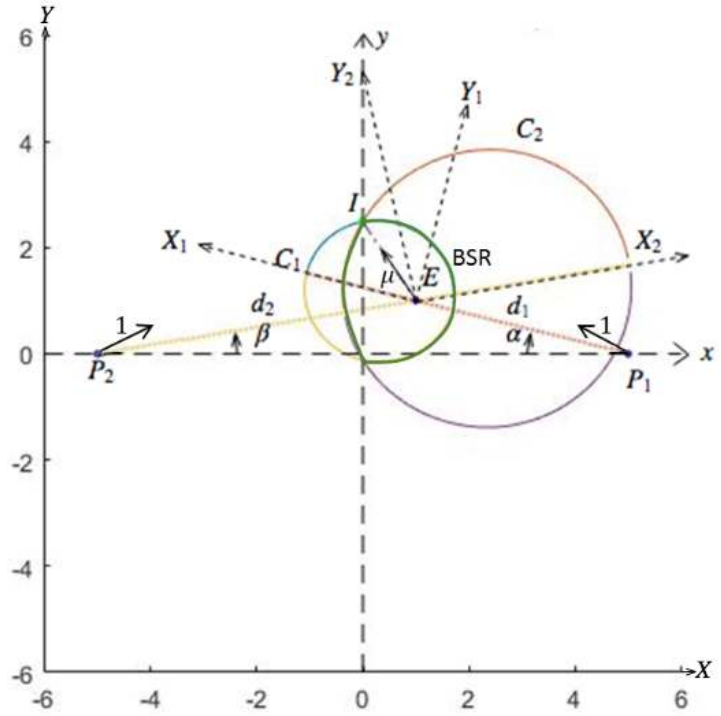

Figure 20: Two Pursuer; $\mu = \frac{1}{2}$, $\frac{l}{d} = \frac{2}{5}$, $x_P = 5$, $x_E = 1$, $y_E = 1$

(X_2, Y_2) where the Apollonius oval C_2 resides is rotated relative to the (x, y) frame by an angle β — see Figure 20 and Equations (30). The transformations take the form of Equations (28) and (29). In the reference frame (x, y) the Apollonius oval C_1 is

$$x_1 = x_E - X_1 \cos\alpha - Y_1 \sin\alpha \ , \quad y_1 = y_E + Y_1 \cos\alpha + X_1 \sin\alpha \tag{28}$$

and the Apollonius oval C_2 is

$$x_2 = x_E - X_2 \cos\beta - Y_2 \sin\beta \ , \quad y_2 = y_E + Y_2 \cos\beta + X_2 \sin\beta \tag{29}$$

where (x_E, y_E) is the evader's instantaneous position in the rotating reference frame (x, y), and α and β are the rotation angles of the axes of P_1 and P_2, respectively. In

terms of the state $(x_P,\, x_E,\, y_E)$, α and β are

$$\begin{aligned} \tan\alpha &= \frac{y_E}{x_P - x_E} \\ \tan\beta &= \frac{y_E}{x_P + x_E} \end{aligned} \tag{30}$$

(X_1, Y_1) is a point of C_1 in the evader-centered frame (X, Y), and (X_2, Y_2) is a point of C_2 in the evader-centered frame (X, Y). In Section 3.2, (X_1, Y_1) and also (X_2, Y_2) were given in an alternative parametric form $X_1 = X_1(\theta_1)$, $Y_1 = Y_1(\theta_1)$ and $X_2 = X_2(\theta_2)$, $Y_2 = Y_2(\theta_2)$ in Equation (**??**) and in Section 3.3 they were given in the parametric form $X_1 = X_1(t_1)$, $Y_1 = Y_1(t_1)$ and $X_2 = X_2(t_2)$, $Y_2 = Y_2(t_2)$ in equations (6). In Equations (6), $d_1 = \sqrt{(x_P - x_E)^2 + y_E^2}$, $d_2 = \sqrt{(x_P + x_E)^2 + y_E^2}$. In the (x, y) frame, C_1 is

$$x_1 = x_1(t_1; x_P, x_E, y_E)\ ,\ y_1 = y_1(t_1; x_P, x_E, y_E)$$

where

$$-\frac{\sqrt{(x_P - x_E)^2 + y_E^2} + l}{1 + \mu} \le t_1 \le \frac{\sqrt{(x_P - x_E)^2 + y_E^2} - l}{1 - \mu}$$

and the Apollonius oval C_2 is

$$x_2 = x_2(t_2; x_P, x_E, y_E)\ ,\ y_2 = y_2(t_2; x_P, x_E, y_E)$$

where

$$-\frac{\sqrt{(x_P + x_E)^2 + y_E^2} + l}{1 + \mu} \le t_2 \le \frac{\sqrt{(x_P + x_E)^2 + y_E^2} - l}{1 - \mu}$$

Because we wish to find the points of intersection of the two ovals in the (x, y) plane, we must obtain two equations for the two unknowns x and y. Concerning the oval C_1, we have

$$(x - x_E)^2 + (y - y_E)^2 = \mu^2 t^2$$

and

$$(x - x_P)^2 + y^2 = (t + l)^2$$

This gives us the equation for C_1

$$[(x - x_P)^2 + y^2 + l^2 - \frac{(x - x_E)^2 + (y - y_E)^2}{\mu^2}]^2 = 4l^2[(x - x_P)^2 + y^2]$$

that is,

$$(x - x_P)^4 + 2(x - x_P)^2[y^2 + l^2 - \frac{(x - x_E)^2 + (y - y_E)^2}{\mu^2}] + [y^2 + l^2 - \frac{(x - x_E)^2 + (y - y_E)^2}{\mu^2}]^2 = 4l^2(x - x_P)^2 + 4l^2y^2 \quad (31)$$

Concerning oval C_2, we have

$$(x - x_E)^2 + (y - y_E)^2 = \mu^2 t^2$$

and

$$(x + x_P)^2 + y^2 = (t + l)^2$$

This gives us the equation for C_2

$$[(x + x_P)^2 + y^2 + l^2 - \frac{(x - x_E)^2 + (y - y_E)^2}{\mu^2}]^2 = 4l^2[(x + x_P)^2 + y^2]$$

that is,

$$(x + x_P)^4 + 2(x + x_P)^2[y^2 + l^2 - \frac{(x - x_E)^2 + (y - y_E)^2}{\mu^2}] + [y^2 + l^2 - \frac{(x - x_E)^2 + (y - y_E)^2}{\mu^2}]^2 = 4l^2(x + x_P)^2 + 4l^2y^2 \quad (32)$$

Equations (31) and (32) yields the ovals' intersection points. However, because the pursuers have the same speed and the same capture radii, by symmetry we conclude that the Apollonius ovals intersect on the y-axis, that is, the x-coordinate of the aimpoint I is $x_I = 0$. This reduces Equations (31) and (32) to the quartic equation in y:

$$x_P^4 + 2x_P^2[y^2 + l^2 - \frac{x_E^2 + (y - y_E)^2}{\mu^2}] + [y^2 + l^2 - \frac{x_E^2 + (y - y_E)^2}{\mu^2}]^2 = 4l^2(x_P^2 + y^2) \quad (33)$$

A quartic equation has 4 roots, giving us 4 possible values for y. The greatest real value for y determines the players' aimpoint I. When $l = 0$, this equation reduces to the quadratic equation

$$x_P^2 + y^2 - \frac{x_E^2 + (y - y_E)^2}{\mu^2} = 0$$

yielding the solution to Isaacs' original Two Cutters and Fugitive Ship differential game. Solving the quadratic equation yields a good initial guess for the iterative solution of the quartic equation, which we note can also be solved analytically.

4.3 Equal Speed Game of Kind

To find the solution to the Game of Kind when the players have equal speed, that is, whether under optimal pursuer play the Evader's capture is guaranteed, we need to determine whether the SR is bounded, which is the case iff the hyperbolae asymptotes intersect. First, the evader must be in between the two pursuers. If the state is outside of the slab $-x_P < x_E < x_P$, the evader can escape. Consider now the diagram in Figure 21. There are four points of interest, O_1,O_2, I', and I'' that are vertices of a quadrilateral. This quadrilateral contains the entirety of the evader's SR, so we can ensure capturability if we determine that this quadrilateral is indeed

formed.

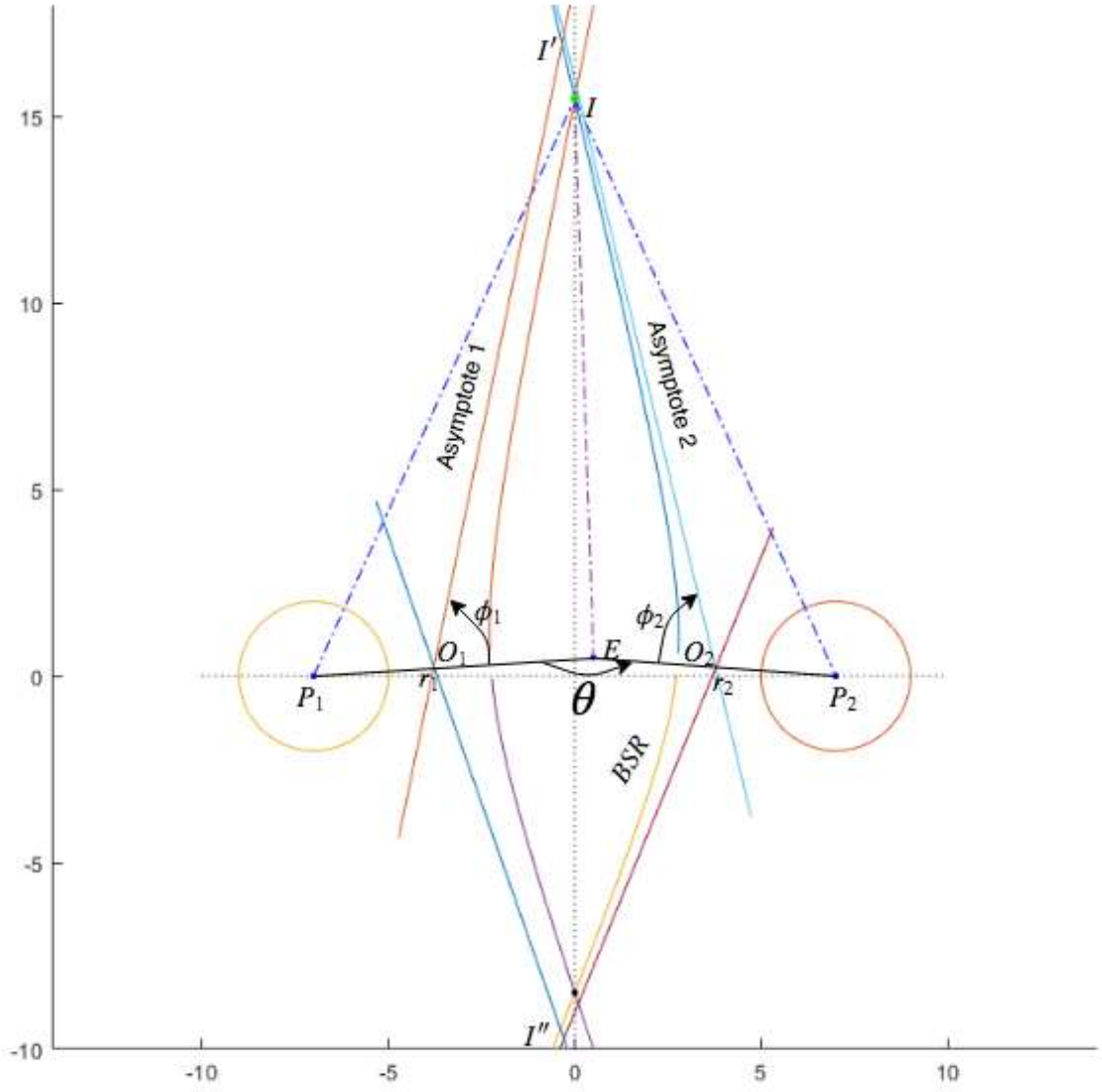

Figure 21: Quadrilateral Formed by Intersecting Asymptotes

To this end, Consider the angles θ, ϕ_1, ϕ_2 in Figure 21. Since a quadrilateral must have all internal angles sum to 360 degrees, we have the following

$$(360 - \theta) + \phi_1 + \phi_2 < 360$$

This yields the condition for a closed SR, and consequently the capturability condition

is

$$\theta > \phi_1 + \phi_2$$

Since the slope of the asymptotes in the realistic plane (X, Y) are specified by Equation 9, we know that $\phi_1 = \arctan(\sqrt{e_1^2 - 1})$ and $\phi_2 = \arctan(\sqrt{e_2^2 - 1})$, with $e_1 = \frac{r_1}{l}$ and $e_2 = \frac{r_2}{l}$. The angles ϕ_1, ϕ_2, and θ are exclusively determined by the game's state (x_P, x_E, y_E). Additionally, we can state that, because both pursuers with equal speed must travel the same distance in the same time, $\Delta I P_1 P_2$ is isosceles, so the vertex I of the BSR must be on the orthogonal bisector of the segment $\overline{P_1 P_2}$; therefore, the intercept point I is on the y-axis. Figure 22 shows the state of this game in the reduced state space (x, y) when P_1, P_2, and E are in a general position. In Figure 22 the points

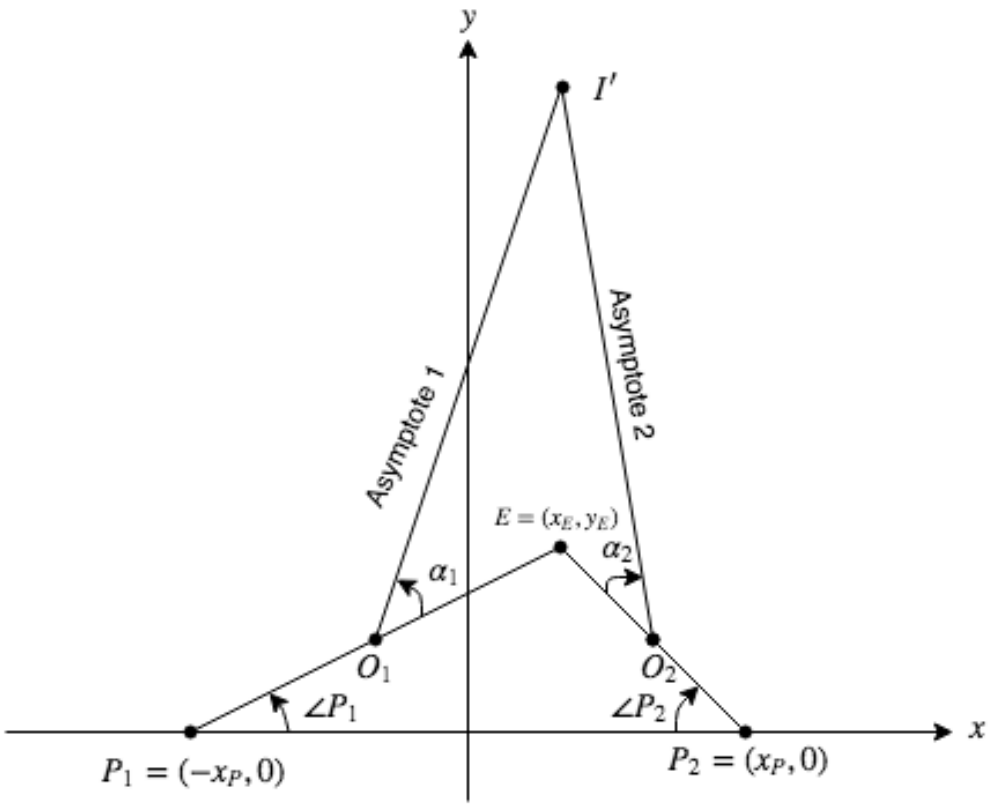

Figure 22: The State (x_P, x_E, y_E)

$$O_1 = \frac{1}{2}(x_E - x_P, y_E) \ , \quad O_2 = \frac{1}{2}(x_E + x_P, y_E)$$

The angles

$$\tan\alpha_1 = \sqrt{e_1^2 - 1} \ , \quad \tan\alpha_2 = \sqrt{e_2^2 - 1}$$

and

$$\tan P_1 = \frac{y_E}{x_P + x_E} \ , \quad \tan P_2 = \frac{y_E}{x_P - x_E}$$

Therefore, summing those angles, we can characterize the captured zone in the reduced state space (x_P, x_E, y_E).

$$\tan(\alpha_1 + P_1) = \frac{y_E + \sqrt{e_1^2 - 1}(x_P + x_E)}{x_P + x_E - y_E\sqrt{e_1^2 - 1}}$$

and

$$\tan(\alpha_2 + P_2) = \frac{y_E + \sqrt{e_2^2 - 1}(x_P - x_E)}{x + P - x_E - y_E\sqrt{e_2^2 - 1}}$$

so

$$\tan(\alpha_1 + P_1) = \frac{ly_E + (x_P + x_E)\sqrt{(x_P + x_E)^2 + y_E^2 - l^2}}{l(x_P + x_E) - y_E\sqrt{(x_P + x_E)^2 + y_E^2 - l^2}}$$

and

$$\tan(\alpha_2 + P_2) = \frac{ly_E + (x_P - x_E)\sqrt{(x_P - x_E)^2 + y_E^2 - l^2}}{l(x_P - x_E) - y_E\sqrt{(x_P - x_E)^2 + y_E^2 - l^2}}$$

The capturability condition then becomes the requirement that the denominator of $\tan(\alpha_1 + P_1) > 0$ and the requirement that the denominator of $\tan(\alpha_2 + P_2) > 0$, as the angles $\alpha_1 + P_1$ and $\alpha_2 + P_2$ would be approaching 90 deg, making the two asymptotes perpendicular to the x-axis and therefore parallel to each other, opening up the SR. We need then

$$l^2(x_p - x_E)^2 > y_E^2[(x_P - x_E)^2 + y_E^2 - l^2]$$

and

$$l^2(x_p + x_E)^2 > y_E^2[(x_P + x_E)^2 + y_E^2 - l^2]$$

which yields the conditions:

$$l^2[(x_p - x_E)^2 + y_E^2] > y_E^2[(x_P - x_E)^2 + y_E^2]$$

and

$$l^2[(x_p + x_E)^2 + y_E^2] > y_E^2[(x_P + x_E)^2 + y_E^2]$$

Fortunately, both of these inequalities are the same and they yield the condition

$$y_E < l$$

This gives us a bound on y_E for where the Evader can be such that the SR would be closed, so under optimal play by the pursuers capture of the evader is possible. Concerning the x-coordinate x_E of E, the condition was given above, that is, the evader is between the two pursuers, that is $-x_P < x_E < x_P$. Therefore, the SR is closed and capturability is guaranteed iff in the reduced state space (x_P, x_E, y_E) the evader is located in the interior of the rectangle in Figure 23. If the x coordinate of the evader is $x_E < -x_P$, $x_E > x_P$ or if the y coordinate is greater than l, then the SR is open and the evader can escape along a straight line path; he might even pre-announce his course and he'll still get away.

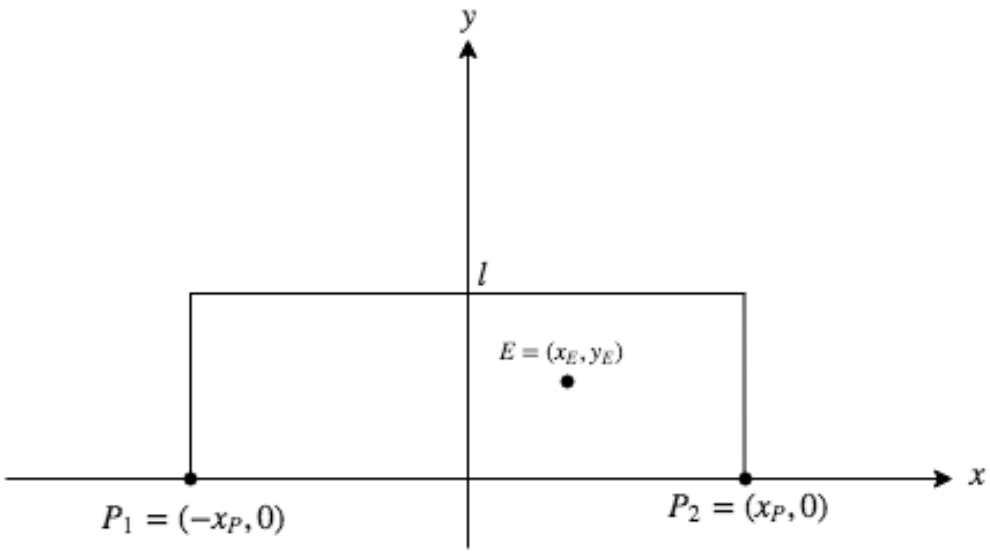

Figure 23: Region of Capture

4.4 Equal Speed Game of Degree

Now that we have ascertained the existence of the surrogate aimpoint, I', we will calculate the players' aimpoint I. The latter is the vertex of the lens shaped BSR which is farther from E. To do so, we must first perform a transformation from the (x, y) frame to the realistic plane (X, Y) by translating and rotating the (x, y) reference frame. Figure 24 shows how the transformation is performed for each pursuer, translating the x and y axes to center upon the evader and rotating the axes such that the evader and the pursuer are on the x axis.

First, we perform a translation to get X_1' and Y_1', centered at point O_1:

$$X_1' = x + \frac{1}{2}(x_P - x_E) \ , \quad Y_1' = y - \frac{1}{2}y_E$$

At this point, we rotate the (x, y) frame so that P_1 and E are on the x-axis.

$$X_1 = X_1' \cos P_1 + Y_1' \sin P_1$$

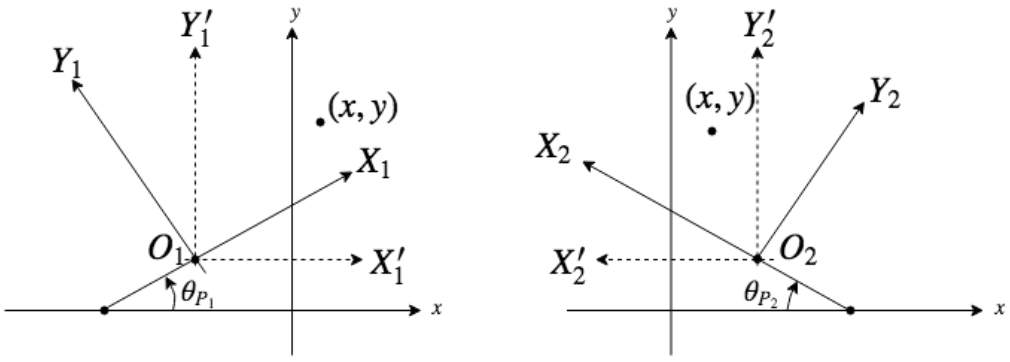

Figure 24: Translation and Rotation

and

$$Y_1 = -X_1' \sin P_1 + Y_1' \cos P_1$$

with

$$\sin P_1 = \frac{y_E}{\sqrt{(x_P + x_E)^2 + y_E^2}} \ , \quad \cos P_1 = \frac{x_P + x_E}{\sqrt{(x_P + x_E)^2 + y_E^2}}$$

Combining the translation and rotation, we have:

$$X_1 = (x + \frac{1}{2}(x_P - x_E)) \cos P_1 + (y - \frac{1}{2} y_E) \sin P_1$$

and

$$Y_1 = -(x + \frac{1}{2}(x_P - x_E)) \sin P_1 + (y - \frac{1}{2} y_E) \cos P_1$$

Substituting values for $\cos P_1$ and $\sin P_1$ into these equations, we have completed the transformation and

$$X_1 = \frac{1}{\sqrt{(x_P + x_E)^2 + y_E^2}} [(x_P + x_E)x + y_E y - \frac{1}{2}(x_E^2 + y_E^2 - x_P^2)] \tag{34}$$

$$Y_1 = \frac{1}{\sqrt{(x_P + x_E)^2 + y_E^2}} [(x_P + x_E)y - y_E x - y_E x_P)] \tag{35}$$

Next, we must also repeat this process for the frame (X_2', Y_2') which is centered at

O_2:

$$X_2' = \frac{1}{2}(x_P + x_E) - x \ , \quad Y_2' = y - \frac{1}{2}y_E$$

At this point, we rotate the x-axis so that P_2 and E are collinear on this axis.

$$X_2 = X_2' \cos P_2 + Y_2' \sin P_2$$

and

$$Y_2 = -X_2' \sin P_2 + Y_2' \cos P_2$$

with

$$\sin P_2 = \frac{y_E}{\sqrt{(x_P - x_E)^2 + y_E^2}} \ , \quad \cos P_2 = \frac{x_P - x_E}{\sqrt{(x_P - x_E)^2 + y_E^2}}$$

Combining the translation and rotation, we have:

$$X_2 = [\frac{1}{2}(x_P + x_E) - x] \cos P_2 + (y - \frac{1}{2}y_E) \sin P_2$$

and

$$Y_2 = -[\frac{1}{2}(x_P + x_E) - x] \sin P_2 + (y - \frac{1}{2}y_E) \cos P_2$$

Substituting values for $\cos P_2$ and $\sin P_2$ into these equations, we have the full description of X_2 and Y_2

$$X_2 = \frac{1}{\sqrt{(x_P - x_E)^2 + y_E^2}}[-(x_P - x_E)x + y_E y - \frac{1}{2}(x_E^2 + y_E^2 - x_P^2)] \tag{36}$$

$$Y_2 = \frac{1}{\sqrt{(x_P - x_E)^2 + y_E^2}}[(x_P - x_E)y + y_E x - y_E x_P)] \tag{37}$$

The (X, Y) frame of reference allows us to use the canonical equations of the hyperbolae,

$$\frac{X_1^2}{a_1^2} - \frac{Y_1^2}{b_1^2} = 1 \ , \quad \frac{X_2^2}{a_2^2} - \frac{Y_2^2}{b_2^2} = 1$$

with

$$a_1 = a_2 = \frac{l}{2}$$

and now

$$b_1 = \frac{1}{2}\sqrt{(x_P + x_E)^2 + y_E^2 - l^2}\ , \quad b_2 = \frac{1}{2}\sqrt{(x_P - x_E)^2 + y_E^2 - l^2}$$

Inserting these expressions into Equations (34)-(37), we obtain

$$\frac{1}{l^2}\frac{[(x_P + x_E)x + y_E y - \frac{1}{2}(x_E^2 + y_E^2 - x_P^2)]^2}{(x_P + x_E)^2 + y_E^2} - \frac{[y_E x - (x_P + x_E)y + x_P y_E]^2}{[(x_P + x_E)^2 + y_E^2][(x_P - x_E)^2 + y_E^2 - l^2]} = \frac{1}{4} \tag{38}$$

and

$$\frac{1}{l^2}\frac{[(x_P - x_E)x - y_E y + \frac{1}{2}(x_E^2 + y_E^2 - x_P^2)]^2}{(x_P - x_E)^2 + y_E^2} - \frac{[y_E x + (x_P - x_E)y - x_P y_E]^2}{[(x_P - x_E)^2 + y_E^2][(x_P + x_E)^2 + y_E^2 - l^2]} = \frac{1}{4} \tag{39}$$

Combining terms, we have:

$$[(x_P+x_E)x+y_E y-\frac{1}{2}(x_E^2+y_E^2-x_P^2)]^2 - l^2\frac{[y_E x - (x_P + x_E)y + x_P y_E]^2}{(x_P - x_E)^2 + y_E^2 - l^2} = \frac{l^2}{4}[(x_P-x_E)^2+y_E^2] \tag{40}$$

and

$$[(x_P-x_E)x-y_E y+\frac{1}{2}(x_E^2+y_E^2-x_P^2)]^2 - l^2\frac{[y_E x + (x_P - x_E)y - x_P y_E]^2}{(x_P + x_E)^2 + y_E^2 - l^2} = \frac{l^2}{4}[(x_P+x_E)^2+y_E^2] \tag{41}$$

However, we know that in the reduced state space $x_I = 0$, so we only need to consider one hyperbola, say hyperbola 1. In Equation (40) set $x = 0$:

$$\frac{[y_E y - \frac{1}{2}(x_E^2 + y_E^2 - x_P^2)]^2}{l^2} - \frac{[(x_P + x_E)y - x_P y_E]^2}{(x_P - x_E)^2 + y_E^2 - l^2} = \frac{1}{4}[(x_P - x_E)^2 + y_E^2] \quad (42)$$

This gives:

$$\frac{[(x_P + x_E)^2 + y_E^2](y_E^2 - l^2)}{l^2[(x_P + x_E)^2 + y_E^2 - l^2]} y^2 - y_E[\frac{[(x_P + x_E)^2 + y_E^2](x_P^2 - x_E^2 + y_E^2 - l^2)}{l^2[(x_P + x_E)^2 + y_E^2 - l^2]}]y +$$
$$\frac{1}{4l^2}(x_E^2 + y_E^2 - x_P^2)^2 - \frac{x_p^2 y_E^2}{(x_P + x_E)^2 + y_E^2 - l^2} - \frac{1}{4}((x_P + x_E)^2 + y_E^2 - l^2) = 0$$

which is a quadratic equation in y. The same equation would have been obtained if we set $x = 0$ in Equation (41) If the state is in the rectangle $\{(x_P, x_E, y_E)| - x_P < x_E < x_P, 0 < y_E < l\}$, the quadratic equation has two real roots. We pick the bigger y.

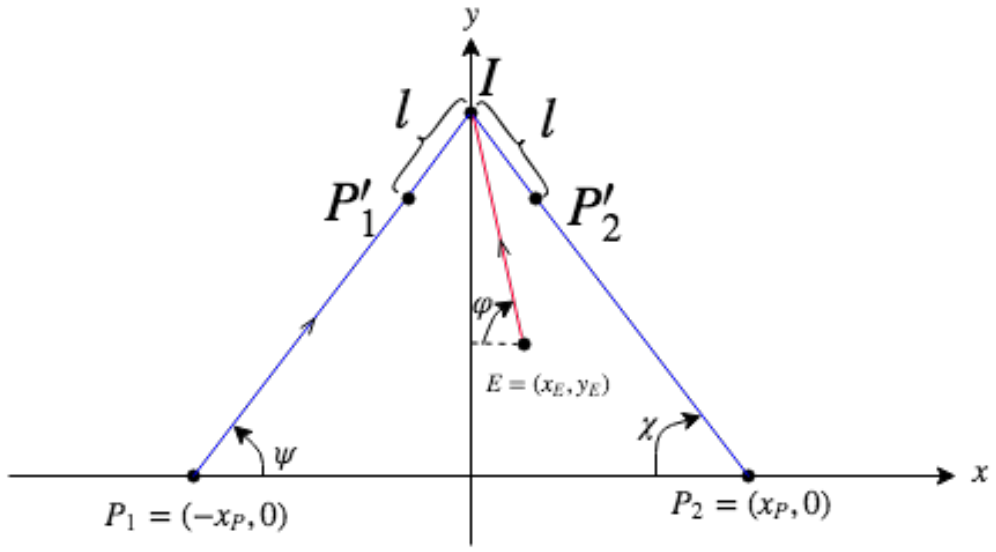

Figure 25: Optimal Headings of the Pursuers and Evader

The players' optimal strategies are — see Figure 25:

$$\psi^* = \arctan(\frac{y(x_P, x_E, y_E)}{x_P}) \ , \quad \chi^* = \arctan(\frac{y(x_P, x_E, y_E)}{x_P}) \ ,$$

$$\varphi^* = \arctan(\frac{y(x_P, x_E, y_E) - y_E}{x_E})$$

and the time-to-go/Value function is

$$V(x_P, x_E, y_E) = \sqrt{[y(x_P, x_E, y_E) - y_E]^2 + x_E^2}$$
$$\forall \ (x_P, x_E, y_E) \ \in \ \{(x_P, x_E, y_E) | -x_P < x_E < x_P, 0 \leq y_E < l\}$$

4.5 Optimization Problem

We can also find the solution via an optimization problem derived as such.

$$X_1(\theta_1; x_P, x_E, y_E) = X_2(\theta_2; x_P, x_E, y_E) \ , \quad Y_1(\theta_1; x_P, x_E, y_E) = Y_2(\theta_2; x_P, x_E, y_E)$$

Inserting Equation (30) in Equation (28), we obtain

$$X_1(\theta_1; x_P, x_E, y_E) \cos(\alpha(x_P, x_E, y_E)) + Y_1(\theta_1; x_P, x_E, y_E) \sin(\alpha(x_P, x_E, y_E)) =$$
$$- X_2(\theta_2; x_P, x_E, y_E) \cos(\beta(x_P, x_E, y_E)) + Y_2(\theta_2; x_P, x_E, y_E) \sin(\beta(x_P, x_E, y_E))$$

and,

$$Y_1(\theta_1; x_P, x_E, y_E) \cos(\alpha(x_P, x_E, y_E)) - Y_2(\theta_2; x_P, x_E, y_E) \cos(\beta(x_P, x_E, y_E))$$
$$= X_2(\theta_2; x_P, x_E, y_E) \sin(\beta(x_P, x_E, y_E)) - X_1(\theta_1; x_P, x_E, y_E) \sin(\alpha(x_P, x_E, y_E))$$

Since x_P, x_E, y_E are fixed, these terms are suppressed and the equations are

$$X_1(\theta_1)\cos\alpha + Y_1(\theta_1)\sin\alpha = -X_2(\theta_2)\cos\beta + Y_2(\theta_2)\sin\beta$$

and,

$$Y_1(\theta_1)\cos\alpha - Y_2(\theta_2)\cos\beta = X_2(\theta_2)\sin\beta - X_1(\theta_1)\sin\alpha$$

that is

$$X_1(\theta_1)\cos\alpha + X_2(\theta_2)\cos\beta + Y_1(\theta_1)\sin\alpha - Y_2(\theta_2)\sin\beta = 0$$

and,

$$Y_1(\theta_1)\cos\alpha + X_1(\theta_1)\sin\alpha - Y_2(\theta_2)\cos\beta - X_2(\theta_2)\sin\beta = 0$$

We must solve these two equations in the two unknowns θ_1 and θ_2. To find the intersection points of the Apollonius ovals, that is, obtain the parameters θ_1 and θ_2, we numerically perform the minimization of the "cost"

$$J_{\theta_1,\theta_2} = \min_{0\le\theta_1\le 2\pi, 0\le\theta_2\le 2\pi}\Big([X_1(\theta_1)\cos\alpha - X_2(\theta_2)\cos\beta + Y_1(\theta_1)\sin\alpha - Y_2(\theta_2)\sin\beta]^2 + [Y_1(\theta_1)\cos\alpha + X_1(\theta_1)\sin\alpha - Y_2(\theta_2)\cos\beta - X_2(\theta_2)\sin\beta]^2\Big)$$

This simplifies to:

$$J_{\theta_1,\theta_2} = \min_{0\le\theta_1\le 2\pi, 0\le\theta_2\le 2\pi}\Big(X_1^2(\theta_1) + Y_1^2(\theta_1) + X_2^2(\theta_2) + Y_2^2(\theta_2) + 2[X_1(\theta_1)X_2(\theta_2) - Y_1(\theta_1)Y_2(\theta_2)]\cos(\alpha+\beta) - 2[X_1(\theta_1)Y_2(\theta_2) + X_2(\theta_2)Y_1(\theta_1)]\sin(\alpha+\beta)\Big) \quad (43)$$

The Apollonius ovals C_1 and C_2 intersect at two points. Solving this optimization, we find the farthest from E intersection point I of the two Apollonius ovals, i.e. the

geometric solution of the differential game, as illustrated in Figure 20.

4.6 Examples

1. Let the problem parameters be $l = 2$ and $\mu = \frac{1}{2}$. Say, the current positions of the players in the reduced state space are $x_P = 5$, $x_E = 1, y_E = 1$ as shown in Figure 20. Therefore, $d_1 = \sqrt{(x_P - x_E)^2 + y_E^2} = \sqrt{18}$ and $d_2 = \sqrt{(x_P + x_E)^2 + y_E^2} = \sqrt{37}$. We calculate $\alpha = \arctan(\frac{1}{4})$ and $\beta = \arctan(\frac{1}{6})$. This gives us the parametric equations for P_1's Apollonius oval C_1 — see Section 3.3,

$$\begin{aligned} X_1(t_1) &= \frac{\frac{3}{4}t_1^2 + 4t_1 - 14}{2\sqrt{18}} \\ Y_1(t_1) &= \sqrt{\frac{1}{4}t_1^2 - \frac{[\frac{3}{4}t_1^2 + 4t_1 - 14]^2}{72}} \quad , \quad -\frac{2+\sqrt{18}}{1.5} \leq t_1 \leq \frac{\sqrt{18}-2}{.5} \end{aligned} \tag{44}$$

Similarly, the parametric equations for the Apollonius oval associated with P_2 are

$$\begin{aligned} X_2(t_2) &= \frac{\frac{3}{4}t_2^2 + 4t_2 - 33}{2\sqrt{37}} \\ Y_2(t_2) &= \sqrt{\frac{1}{4}t_2^2 - \frac{[\frac{3}{4}t_2^2 + 4t_2 - 33]^2}{148}} \quad , \quad -\frac{2+\sqrt{37}}{1.5} \leq t_2 \leq \frac{\sqrt{37}-2}{.5} \end{aligned} \tag{45}$$

Since the state is in the region $R_{1,2}$ upon reverting to the (x, y) frame — see Figure 19 — Eq. (33) is solved to yield the aimpoint I on the y-axis. This equation lends us 4 solutions, two of which are the intersection points of our two Apollonius ovals. As the pursuers are on the x-axis, the longer path would be the path with a greater absolute value on the y-axis.

The aimpoint I in Figure 20 is calculated for $x_P = 5$, $x_E = 1$, $y_E = 1$, the speed ratio $\mu = \frac{1}{2}$, and $l = 2$ to be at $I = (0, 2.4873)$. Hence, we calculate the players'

optimal headings — see Figure 16: the heading of P_2 is ψ^*, of P_1 is χ^*, of E is φ^*:

$$\begin{aligned} \varphi^* &= \arctan(\frac{y_I - y_E}{x_I - x_E}) \\ \psi^* &= \arctan(\frac{y_I}{-x_P - x_I}) \\ \chi^* &= \arctan(\frac{y_I}{x_P - x_I}) \end{aligned} \tag{46}$$

For the current state $x_P = 5$, $x_E = 1$, and $y_E = 1$, we find these to be:

$$\varphi^* = 124.0\,\text{deg}$$

$$\psi^* = 26.4\,\text{deg}$$

$$\chi^* = 153.5\,\text{deg}$$

2. Consider the case where the pursuers are only slightly faster than the evader, that is, the speed ratio is $\mu = 1$; $l = 2.5$. Let's also set the players' initial positions at $x_P = 5$, $x_E = .25$, and $y_E = .5$. When the speed ratio is 1 the BSR is a hyperbola — see Figure 9. We then proceed as in the first case to find the aimpoint I of the players. Similar to the previous case, we first calculate the distance between the pursuers and the evader, $d_1 = \sqrt{(x_P - x_E)^2 + y_E^2} = \sqrt{22.8125}$ and $d_2 = \sqrt{(x_P + x_E)^2 + y_E^2} = \sqrt{27.8125}$, with the angles $\alpha = \arctan(\frac{1}{9.5})$ and $\beta = \arctan(\frac{1}{10.5})$. We then obtain the following parametric equations for each of the two hyperbolae.

$$\begin{aligned} X_1(t_1) &= \frac{5t_1 - 16.5625}{2\sqrt{22.8125}} \\ Y_1(t_1) &= \sqrt{t_1^2 - \frac{[5t_1 - 16.5625]^2}{91.25}} \quad , \quad -\frac{2.5 + \sqrt{22.8125}}{2} \leq t_1 \leq \inf \end{aligned} \tag{47}$$

Likewise,

$$X_2(t_2) = \frac{5t_2 - 21.5625}{2\sqrt{27.8125}}$$
$$Y_2(t_2) = \sqrt{t_2^2 - \frac{[5t_2 - 21.5625]^2}{111.25}} \quad , \quad -\frac{2.5 + \sqrt{27.8125}}{2} \leq t_2 \leq \inf \tag{48}$$

The bounds on the possible values for t_1 and t_2 go up to infinity as the SR for each evader-pursuer pairing in this case is unbounded. However, the composite BSR is bounded because the state is such that the asymptotes to the hyperbolae intersect. Reverting to the (x, y) frame, setting $x_I = 0$ and calculating y_I, now forces the solution of a quadratic equation in lieu of the quartic Eq. (33). We find the aimpoint to be $I = (0, 5.662)$, as seen in Fig. 26.

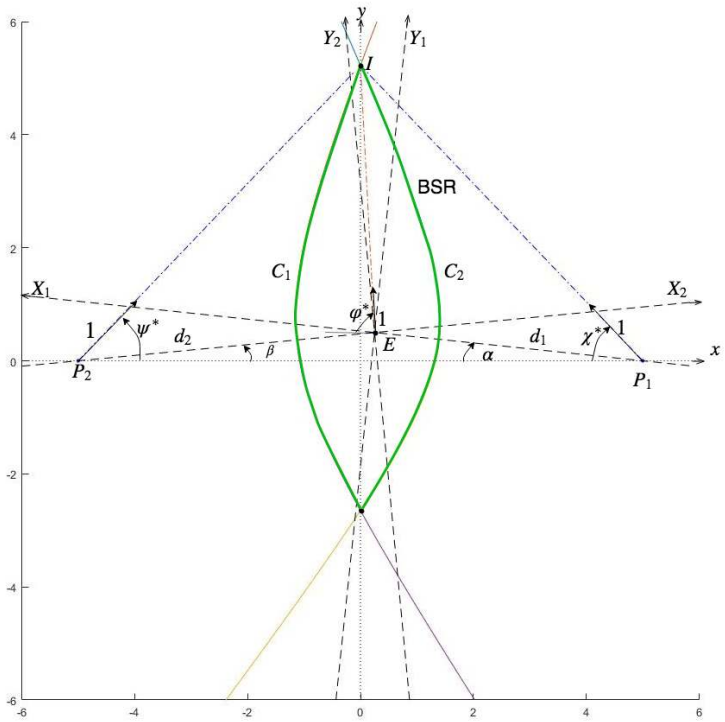

Figure 26: Case 2 Figure

For the current state $x_P = 5$, $x_E = .25$, and $y_E = .5$ and $\mu = 1$, we find the

players' optimal heading angles to be, as per Equations (46),

$$\varphi^* = 93.0\,\text{deg}$$

$$\chi^* = 46.3\,\text{deg}$$

$$\psi^* = 133.7\,\text{deg}$$

3. Now we will evaluate this for the case where the pursuers have different speeds so the speed ratios are $\mu_1 = \frac{1}{2}$, $\mu_2 = 1$; $l = 2.5$. Let's also set the player's initial positions at $x_P = 5$, $x_E = .25$, and $y_E = .5$. We see in Figure 9 that the BSR when the speed ratio is 1 is a hyperbola. As the two pursuers have different speeds, we cannot use the methods given above. Therefore, we solve the optimization given in Equation (43) to find what the aimpoint of the players should be. Similar to the previous cases, we first calculate the distance between the pursuers and the evader, $d_1 = \sqrt{(x_P - x_E)^2 + y_E^2} = \sqrt{22.8125}$ and $d_2 = \sqrt{(x_P + x_E)^2 + y_E^2} = \sqrt{27.8125}$. The angles of each $\alpha = \arctan(\frac{1}{9})$ and $\beta = \arctan(\frac{1}{11})$. Then, like in the first case, we see similar parametric equations, but the speeds and distances will be different this time.

$$\begin{aligned} X_1(t_1) &= \frac{\frac{3}{4}t_1^2 + 5t_1 - 14.25}{2\sqrt{20.5}} \\ Y_1(t_1) &= \sqrt{\frac{1}{4}t_1^2 - \frac{[\frac{3}{4}t_1^2 + 5t_1 - 14.25]^2}{82}} \quad , \quad -\frac{2.5 + \sqrt{20.5}}{1.5} \leq t_1 \leq \frac{\sqrt{20.5} - 2.5}{.5} \end{aligned} \tag{49}$$

Likewise,

$$\begin{aligned} X_2(t_2) &= \frac{5t_2 - 24.25}{2\sqrt{30.5}} \\ Y_2(t_2) &= \sqrt{t_2^2 - \frac{[5t_2 - 24.25]^2}{122}} \quad , \quad -\frac{2.5 + \sqrt{37}}{2} \leq t_2 \leq \inf \end{aligned} \tag{50}$$

The bounds on the possible values for t_2 in Equation (50) go up to infinity as the BSR

in this case is unbounded. However, the BSR described by Equation (49) is bounded, meaning that the effective BSR is bounded. This will be true so long as the radius of capture does not equal the distance between the pursuer and evader. Performing the optimization, we find the aimpoint to be $I = (-0.97, 1.61)$ as seen in 26.

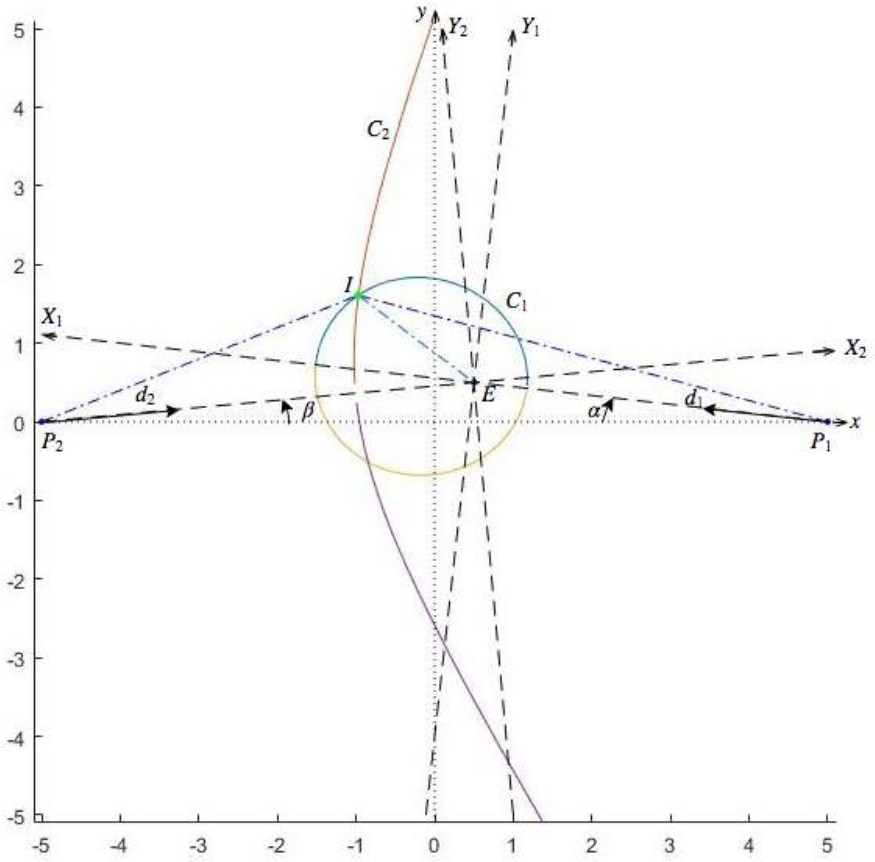

Figure 27: Case 3 Figure

For the current state $x_P = 5$, $x_E = .5$, and $y_E = .5$ and $\mu_1 = .5$, $\mu_2 = 1$, we find the players' heading angles to be, as per Equation (46)

$$\varphi^* = 143.0\,\text{deg}$$

$$\chi^* = 15.1\,\text{deg}$$

$$\psi^* = 158.2\,\text{deg}$$

These calculations must be performed in real time as the (reduced) state of the game changes over time.

During optimal play the frame (x, y) is not rotating and the players' optimal trajectories in the realistic plane and in the reduced state space are straight lines. In summary, the following holds

Theorem 1. *The two-on-one pursuit-evasion differential game where the pursuers are endowed with a capture radius $l > 0$ and the speed ratio $\frac{v_E}{v_P} = \mu < 1$ is considered. The solution of the Game of Kind is given by the surface (27) which delimits the region where both pursuers cooperatively and isochronously capture the evader. The Game of Degree is then solved by finding the optimal aimpoint of the three players: When the pursuers have equal speed and equal capture radii, this entails the solution in real time of a quartic equation, Eq. (33). When the pursuer have different speeds or have different capture radii, this will require the solution of a system of two polynomial equations of degree four with two variables, Equations (31) and (32). And when all the players have the same speed and the pursuers have equal capture radii the capturability region is bounded. When the state is in the capturability region the solution of the game of Degree entails the solution of a quadratic equation.* □

V. Conclusion

The two-on-one pursuit-evasion differential game where the three players have simple motion à la Isaacs and the two pursuers are endowed with a radius of capture $l > 0$ is solved. We provided the solution of the Game of Kind by obtaining the partitioning of the state space into the respective regions R_1, R_2 and $R_{1,2}$ illustrated in Figure 19, where pursuer P_1 captures the evader single-handedly, pursuer P_2 captures the evader single-handedly, and both pursuers P_1 and P_2 cooperatively and isochronously capture the evader. The surface separating the three capture zones is similar to the planar surface when the pursuers' capture radius $l = 0$, as expected, but becomes more curved as l increases, with the region $R_{1,2}$ shrinking as l increases. The Game of Degree was solved using Isaacs' geometric method. To this end, first the Apollonius ovals which are a departure from the classical Apollonius circle were constructed. Having a finite radius of capture did reduce the size and altered the shape of the Apollonius ovals, but, of course, the equations derived hold for the classical limiting case $l = 0$ where we have Apollonius circles. When the capture range $l > 0$, the solution of the Game of Degree, that is, the calculation of the optimal state feedback strategies, necessitates the real time analytic solution of a quartic equation — this, as opposed to the limiting case of point capture where $l = 0$ and the solution of the Game of Degree came down to the solution of a quadratic equation. However, similar to the case of point capture, in this two-on-one differential game, when $l > 0$, the players' optimal trajectories in both the realistic plane and in the reduced state space are straight lines. The optimal flow field then consists of straight lines. This is a three state differential game with primary optimal trajectories and regular characteristics only. There are no singular surfaces and the Value function is differentiable. Thus, the solution of this differential game is identical to the solution of the two-sided max min optimal control problem.

Bibliography

1. R. Isaacs, *Differential games : a mathematical theory with applications to warfare and pursuit, control and optimization*. Dover Publications, 1999.

2. M. Pachter, "Isaacs' Two-on-One Pursuit Evasion Game," in *ISDG*, 2018.

3. A. W. Merz, "The Homicidal Chauffeur - A Differential Game," 1971. [Online]. Available: http://www.dtic.mil/docs/citations/AD0885270

4. L.S. Pontriagin and L. W. Neustadt, *The mathematical theory of optimal processes*. Gordon and Breach Science Publishers, 1986.

5. R. Bellman, "Dynamic programming." *Science (New York, N.Y.)*, vol. 153, no. 3731, pp. 34–7, jul 1966. [Online]. Available: http://www.ncbi.nlm.nih.gov/pubmed/17730601

6. A. Perelman, T. Shima, and I. Rusnak, "Cooperative Differential Games Strategies for Active Aircraft Protection from a Homing Missile," *Journal of Guidance, Control, and Dynamics*, vol. 34, no. 3, 2011.

7. T. Mylvaganam, M. Sassano, and A. Astolfi, "A Differential Game Approach to Multi-agent Collision Avoidance," *IEEE Transactions on Automatic Control*, 2017.

8. J. V. Breakwell and P. Hagedorn, "Point capture of two evaders in succession," *Journal of Optimization Theory and Applications*, vol. 27, no. 1, pp. 89–97, jan 1979. [Online]. Available: http://link.springer.com/10.1007/BF00933327

9. E. Garcia, D. W. Casbeer, K. Pham, and M. Pachter, "Cooperative aircraft defense from an attacking missile," in *Proceedings of the IEEE Conference on Decision and Control*, vol. 2015-Febru, no. February, 2014.

10. S. Rubinsky and S. Gutman, "Three-Player Pursuit and Evasion Conflict," *Journal of Guidance, Control, and Dynamics*, vol. 37, no. 1, 2014.

11. S. Kang, H. J. Kim, and M.-J. Tahk, "Aerial Pursuit-Evasion Game Using Nonlinear Model Predictive Guidance," in *AIAA Guidance, Navigation, and Control Conference*. Reston, Virigina: American Institute of Aeronautics and Astronautics, aug 2010. [Online]. Available: http://arc.aiaa.org/doi/10.2514/6.2010-7880

12. K. Horie and B. A. Conway, "Optimal Fighter Pursuit-Evasion Maneuvers Found Via Two-Sided Optimization," *Journal of Guidance, Control, and Dynamics*, vol. 29, no. 1, pp. 105–112, jan 2006. [Online]. Available: http://arc.aiaa.org/doi/10.2514/1.3960

13. P. Wasz, M. Pachter, and K. Pham, "No Title," in *submitted to the Mediterranean Conference on Control and Automation*, 2019, p. 6.

REPORT DOCUMENTATION PAGE

Form Approved
OMB No. 0704–0188

1. REPORT DATE *(DD–MM–YYYY)*	2. REPORT TYPE	3. DATES COVERED *(From — To)*
03–21–2019	Master's Thesis	Sept 2017 — Mar 2019

4. TITLE AND SUBTITLE

TWO-ON-ONE PURSUIT WITH
A NON-ZERO CAPUTURE RADIUS

5a. CONTRACT NUMBER

5b. GRANT NUMBER

5c. PROGRAM ELEMENT NUMBER

6. AUTHOR(S)

Wasz, Patrick J, 2d Lt, USAF

5d. PROJECT NUMBER

5e. TASK NUMBER

5f. WORK UNIT NUMBER

7. PERFORMING ORGANIZATION NAME(S) AND ADDRESS(ES)

Air Force Institute of Technology
Graduate School of Engineering an Management (AFIT/EN)
2950 Hobson Way
WPAFB OH 45433-7765

8. PERFORMING ORGANIZATION REPORT NUMBER

AFIT/ENG/19M

9. SPONSORING / MONITORING AGENCY NAME(S) AND ADDRESS(ES)

AFRL/RV
3550 Aberdeen Avenue SE Bldg 427
Kirtland AFB, NM 87117-5776
COMM 850-882-4033
Email: robert.murphey@us.af.mil

10. SPONSOR/MONITOR'S ACRONYM(S)

AFRL/RV

11. SPONSOR/MONITOR'S REPORT NUMBER(S)

12. DISTRIBUTION / AVAILABILITY STATEMENT

DISTRIBUTION STATEMENT A:
APPROVED FOR PUBLIC RELEASE; DISTRIBUTION UNLIMITED.

13. SUPPLEMENTARY NOTES

14. ABSTRACT

A revisiting of the "Two Cutters and Fugitive Ship" differential game that was solved by Isaacs, but moving away from point capture. We consider a two-on-one pursuit-evasion differential game with simple motion and pursuers endowed with circular capture sets of radius $l > 0$. The regions in the state space where only one pursuer effects the capture and the region in the state space where both pursuers cooperatively and isochronously capture the evader are characterized, thus solving the Game of Kind. Concerning the Game of Degree, the algorithm for the synthesis of the optimal state feedback strategies of the cooperating pursuers and of the evader is presented.

15. SUBJECT TERMS

Differential Games, Controls, Optimization

16. SECURITY CLASSIFICATION OF:			17. LIMITATION OF ABSTRACT	18. NUMBER OF PAGES	19a. NAME OF RESPONSIBLE PERSON
a. REPORT	b. ABSTRACT	c. THIS PAGE			Dr. Meir Pachter, AFIT/ENG
U	U	U	UU	67	19b. TELEPHONE NUMBER *(include area code)* (937) 255-3636, x7247; meir.pachter@afit.edu